Analytical one-particle approach to the π electronic structure of heterocyclic polymers

Alexander Onipko[a)]
Department of Physics and Measurement Technology, Linköping University, S-581 83 Linköping, Sweden

Yuriy Klymenko
Space Research Institute, Kiev, 252022, Ukraine

Lyuba Malysheva
Bogolyubov Institute for Theoretical Physics, Kiev, 252143, Ukraine

(Received 6 May 1997; accepted 30 June 1997)

The one-electron description of heterocyclic five-membered ring polymers is derived on the basis of the Su–Schrieffer–Heeger–Hückel type Hamiltonian which accounts for the electronic interaction of the heteroatom p-orbital lone pair with the π band structure of the carbon backbone. An explicit form of the fifth order equation, the solutions of which determine the dispersion relations for five π electron bands and closed expressions of molecular orbitals, is obtained. The main accent is put on the gross π electronic polymer structure. It is shown that there exists one-to-one correspondence between the structure considered as a function of basic system parameters [such as the electron on-site energies at carbon (C) and heteroatom (X), and resonance integrals associated with C–C and X–C bonds] and zeros of the Green function of polymer building blocks—monomers. This interrelation is expressed in the form of certain equations for the monomer Green function matrix elements, which predict the values of system parameters at which the π electron spectrum contains closed gaps (some bands join each other), in-gap states, and degenerate bands. Ten band-edge energies of five π bands of heterocyclic polymers are found as analytical functions of system parameters. Four of 10 band-edge energies are shown to be independent of heteroatom parameters due to the system symmetry. The heteroatom effects on the band edges are traced for polythiophene, polypyrrole, and polyfuran. Theoretical results are compared with available experimental data, and band gaps and bandwidths of π electrons in heterocyclic polymers are predicted. [S0021-9606(97)51937-4]

I. INTRODUCTION

During the past 15 years the π electronic structure of conjugated polymers and oligomers based on five-membered ring heterocycles has been the subject of a considerable theoretical effort[1–16] fed by an enormous amount of experimental work. The great interest to this family of conducting polymers is stimulated by wide possibilities of their use as electronic materials due to the comparatively small intrinsic band gap, good conductivities upon doping, and improved environmental stability and processing.

Most of calculations were concerned with the fundamental band gap,[2–7,9,10,12–16] and there are few papers where the full π electron spectrum is discussed.[1,8,11] The first reported theoretical values of the gap[1,8] were much larger than those observed experimentally. With the improvement of calculation schemes a much better agreement between the theory and experiment has been achieved.[3,10,16] Also, the underlying physics that rules the gap formation has been clarified in great detail.

Unlike polyacetylene, in conjugated polymers based on aromatic rings the band gap is not minimal, if carbon–carbon bond alternation (the Peierls distortion) is equal to zero. Brédas[3] was the first who showed that in these polymers ''the band gap decreases as a function of increasing quinoid character of the (carbon) backbone.'' It was also claimed that ''the intrinsic gap can never completely close because these bands belong to the same irreducible representation.'' Physical explanations of the former effect were given by Mintmire *et al.*[7] and were further detailed by Lee and Kertesz.[10] However, the impossibility of joining the bands has been opposed by both groups of authors.

According to Mintmire *et al.*[7] the decrease of the gap in the five-membered ring polymers with the increase of the quinoid character of the parent *cis*-polyacetylene chain can be easily understood if the symmetry of frontier states of the latter is taken into account. These states described by the highest occupied molecular orbital (HOMO) and lowest unoccupied molecular orbital (LUMO) have wave vectors at $k=0$ in the one-dimensional Brillouin zone and preserve the local symmetry of the monomer, i.e., within each monomer the wave function is symmetric or antisymmetric with respect to the reflection in the plain perpendicular to the chain and contain an heteroatom in this plane. From these two the antisymmetric state has lower one-electron energy and thus, it corresponds to HOMO, while the symmetric state corresponds to LUMO, if the backbone has the aromatic structure (see Fig. 1). In the case of quinoid geometry, the situation is just reversed. Since $pp\pi$ interaction between the heteroatom and carbon (X–C resonance interaction) affects the symmet-

a)Electronic mail: alex@ifm.liu.se

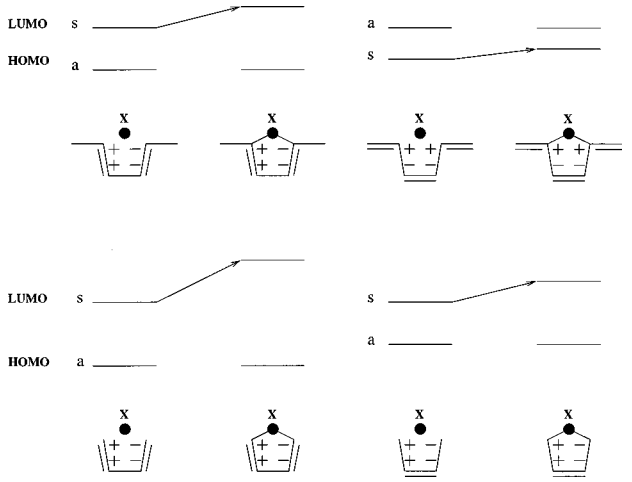

FIG. 1. Effect of heteroatom–carbon resonance interaction on HOMO and LUMO levels in five-membered ring monomer (down) and corresponding polymer (up). In monomer, HOMO is antisymmetric (a) in both aromatic (left) and quinoid (right) conformations; in polymer, HOMO is antisymmetric in aromatic conformation but symmetric (s) in quinoid conformation. Accordingly to Mintmire *et al.* (see Ref. 7), this leads to a qualitative changing of heteroatom effect on HOMO-LUMO gap in the cases of aromatic and quinoid geometry of polymer backbone. Phases of MO coefficients at carbons are shown by + and −.

ric state and has no effect on the antisymmetric one, and since the energy of the heteroatom lone orbital (X level) is always anticipated to be below LUMO and HOMO levels of *cis*-polyacetylene, one comes to the conclusion that the effect produced by $X-C$ interaction on the aromatic form of *cis*-polyacetylene leads to the band gap increase, but to the decrease, if the carbon chain has quinoid structure, as shown schematically in Fig. 1. In the picture given by Mintmire *et al.*,[7] there are no restrictions which prevent the band gap from closing (i.e., touching of the top and bottom of HO and LU bands, respectively) at a certain degree of the quinoid character of carbon backbone. This point has been accepted in a later publications of Brédas *et al.*[6] and Brédas,[9] which give a convincing illustration of practical applications of the quantum chemistry aided design of organic polymers.

More importantly, the symmetry interchange between HOMO and LUMO states, when passing from the aromatic to quinoid form of the carbon backbone, occurs only in polymers. (An effective increase of the quinoidlike contribution to the electronic structure of aromatic ring based polymers associates with *n* or *p* type doping;[2] it can also be attained by certain types of substitution.[9]) Such an interchange does not take place in a five-membered ring monomer, where HOMO is antisymmetric and LUMO symmetric with respect to the symmetry operation indicated above, independent of the monomer form (see Sec. III). Therefore, the $\pi-\pi^*$ gap of a heterocyclic ring is always expected to be larger than that of the monomer of *cis*-polyacetylene which consists of four CH units (see Fig. 1).

From the above observation it immediately follows that at least three factors have to be considered simultaneously, to understand the trends in HOMO-LUMO gap of heterocyclic ring based polymers. These are:

(i) the character (aromatic or quinoid) of C–C bond alternation;
(ii) the pure electronic $X-C$ interaction (both heteroatom parameters, the π electron on-site energy and the $X-C$ resonance interaction are important); and
(iii) the intermonomer resonance interaction.

The latter certainly associates but is not completely determined by the bond length between carbons of different rings in alpha positions ($C_\alpha-C_{\alpha'}$). Therefore, the given alternation of carbon–carbon bonds does not necessarily implies a certain relation between the C–C resonance interaction within the ring and between rings. Apart from the C–C bond length the intermonomer interaction is also dependent on the torsion angle between adjacent rings of the polymer, since twisting by some angle relative to each other leads to the decrease of conjugation and thus, modifies the electronic structure of the polymer.[4,12] So, for the fixed character of carbon backbone (either aromatic or quinoid) one can expect different heteroatom effects on the π electron spectrum which will be highlighted in this presentation.

The resonance interaction between alpha carbons within the ring also gives a substantial contribution to the gap energy[14,16] enlarging the number of most important factors up to four. Of course these same factors play the dominant role in determining all other characteristics of the π electron spectrum such as band gaps other than the fundamental one, band widths, etc., which thus far have received much less attention. Hence, it is desirable to extend the understanding achieved with respect to the fundamental gap to the full π electron spectrum.

The main objective of this work is to clarify the specific role of each of the above mentioned factors in the formation of π electronic structure of heterocyclic polymers and oligomers within a simple physical model, which allows one to examine analytically the main results obtained in numerical calculations and to gain insight into their physical origins.

In particular, it will be shown that all band-edge energies can be expressed in a closed form. Precisely, those of them which do not contain parameters of heteroatom, i.e., the band-edge energies of *cis*-polyacetylene not affected by heteroatoms, are represented by solutions of two second order equations, whereas those which are affected are represented by solutions of two third order equations. Two of the ten band-edge energies, one dependent on the heteroatom parameters and another one independent of them, correspond to the HOMO and LUMO energies. Since they are obtained as explicit functions of system characteristic parameters, all previous results concerning the fundamental gap dependence on these parameters are restored and some new aspects of this dependence as well as analogous dependences related to other π electron bands are discussed.

Special attention will be paid to the striking feature possessed by the spectrum of five-membered ring polymers, but not observed in six-membered ring polymers—the band degeneracy which is not connected with zero π electron density at binding sites (i.e., alpha carbons) of monomer. The effect of the band (not gap) closing can be conceived, if one of the

band edges of the parent carbon chain is repulsed by heteroatoms towards the opposite band edge of the same band, which is not affected by heteroatoms. Examining the possibility of such an event (again, connected with the system symmetry) and its manifestations in the electronic spectrum of heterocyclic polymers is among the particular tasks of the present analysis.

Although the neglect of electron–electron interaction is never justified in a many-electron system, the one-electron approximation used here is recognized to be adequate for understanding a number of fundamental properties of conducting polymers.[17] The Su–Schrieffer–Heeger (SSH) model,[18] which treats the π electron subsystem in terms of the tight-binding nearest-neighbor approximation and the σ electrons—adiabatically, has proven to be one of the most successful descriptions of the essentials of excited and charge carrying states of conducting polymers. In this work we use the SSH model with its π electronic part appropriately modified for heterocyclic polymers and with the further simplification assuming the rigid geometry of the oligomer/polymer backbone. This crude approximation puts outside the present discussion the polaron and bipolaron states.[19–23] Obviously, the polaronic effects as well as the problem of the insulator/metal transition in conducting polymers[24–27] cannot be approached without the electron–phonon coupling being taken into account. Still, some insight into the doping effects can also be made by analyzing the gap, valence, and conduction band behavior as a function of the quinoid character of carbon backbone.[2,3] In this respect, the use of analytical results obtained here presents certain advantages in comparison with numerical calculations.

It is also worth mentioning that our analysis is started from the oligomer level, and the polymer spectrum is obtained in the limit of infinite oligomer length. Of course, the gross structure of π electron spectrum of infinite chain does not depend on whether the periodic boundary conditions or the terminated (free end) chain model is used. However, in the latter model, which is closer in spirit to real polymeric materials consisting of long chain segments but not chain rings, the end effects are taken strictly into account. These are shown to be very likely to reveal themselves as in-gap discrete states of heterocyclic polymers/oligomers especially in the case of the quinoid geometry.

The structure of this article is as follows. In Sec. II we introduce the model and derive general relations which describe one-electron spectrum and wave functions of molecules with structure $M-M-\cdots-M$ in terms of the Green function of building blocks M. In Sec. III these relations (including equations which determine the band-edge energies, local state spectrum, and energies of band degeneracy) are specified by using explicit expressions of Green function matrix elements of five-membered heterocycle. The closed expressions of orthonormalized molecular orbitals of heterocyclic oligomers/polymers are also obtained. Section IV gives visual representation of main heteroatom effects by means of illustrative calculations with the use of different sets of heteroatom parameters taken from the literature. The latter section also presents data on band gaps, band widths, etc., which are compared with experimental results and theoretical predictions obtained by numerical methods. Section V briefly summarizes the main results of this work.

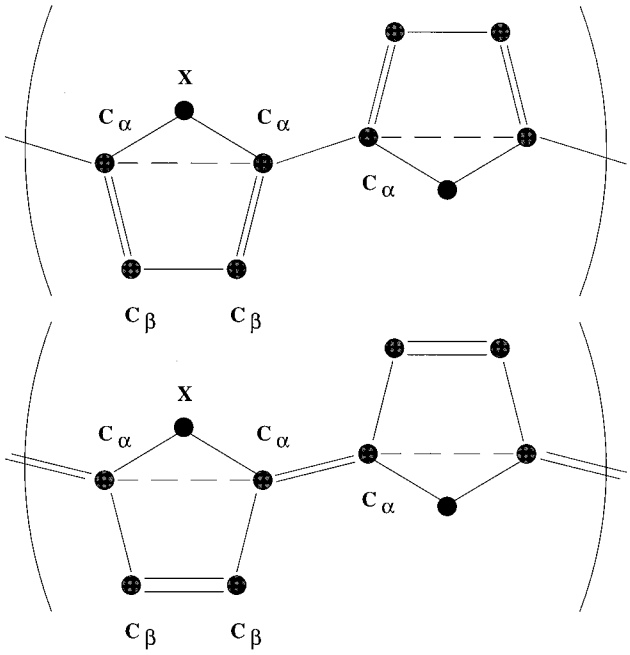

FIG. 2. Aromatic (up) and quinoid (down) geometry of five-membered-ring based polymers: polythiophene ($X=$S), polypyrrole ($X=$NH), and polyfuran ($X=$O). In the given model single and double C—C bonds within rings and between rings associate with different resonance integrals. An additional resonance interaction between alpha carbons within rings (indicated by interrupted line) is described by parameter γ. For the convenience of comparison with spectrum and wave functions of *cis*-polyacetylene (unperturbed parent carbon chain) we consider polymer chain as having one ring per elementary cell.

II. MODEL: GENERAL CONSIDERATION

The π electronic part of the SSH Hückel type Hamiltonian which describes an oligomer consisting of N heterocyclic rings $H-(C_4H_2X)_N-H$ (where $X=$S, NH, or O in oligomers of polythiophene, polypyrrole, or polyfuran, respectively) has the form

$$H=\sum_{n,n'=1}^{N}\sum_{\mathbf{r}_1,\mathbf{r}_2} H_{n_{\mathbf{r}_1},n'_{\mathbf{r}_2}}|n_{\mathbf{r}_1}\rangle\langle n'_{\mathbf{r}_2}|. \tag{1}$$

In Eq. (1), n and n' denote the number of monomers in the chain; $\mathbf{r}_1$ and $\mathbf{r}_2$ stand for coordinates of atoms within the five-membered ring: the left (l), right (r) carbons in alpha ($\mathbf{r}_{\alpha_{l,r}}$) and beta ($\mathbf{r}_{\beta_{l,r}}$) positions, and heteroatom ($\mathbf{r}_X$) (see Fig. 2) ket and bra vectors have the usual meaning $|n_{\mathbf{r}}\rangle \equiv c^+_{n_{\mathbf{r}}}|0\rangle$ and $\langle n_{\mathbf{r}}|\equiv\langle 0|c_{n_{\mathbf{r}}}$, where $|0\rangle$ is the vacuum wave function, and $c^+_{n_{\mathbf{r}}}$ ($c_{n_{\mathbf{r}}}$) is the Fermi operator which creates (destroys) π electrons of spin $\pm\frac{1}{2}$ on the $\mathbf{r}$th atom of the nth monomer (electron spin variables are omitted for simplicity); and $H_{n_{\mathbf{r}_1},n'_{\mathbf{r}_2}}=\delta_{n,n'}H^M_{\mathbf{r}_1,\mathbf{r}_2}+(1-\delta_{n,n'})V_{n_{\mathbf{r}_1},n'_{\mathbf{r}_2}}$ is the Hückel Hamiltonian matrix defined as

$$H^M_{\mathbf{r}_1,\mathbf{r}_2}=\beta\begin{cases}\epsilon_X, & \text{if } \mathbf{r}_1=\mathbf{r}_2=\mathbf{r}_X\\ \beta_{\mathrm{C}-X}/\beta\equiv\gamma_X, & \text{if } \mathbf{r}_1=\mathbf{r}_{\alpha_l},\mathbf{r}_{\alpha_r},\ \mathbf{r}_2=\mathbf{r}_X;\ \mathbf{r}_1\leftrightarrow\mathbf{r}_2\\ \beta_{\mathrm{C=C}}/\beta=e^{\eta}, & \text{if } \mathbf{r}_1=\mathbf{r}_{\alpha_l},\ \mathbf{r}_2=\mathbf{r}_{\beta_l};\ \mathbf{r}_1=\mathbf{r}_{\alpha_r},\ \mathbf{r}_2=\mathbf{r}_{\beta_r};\ \mathbf{r}_1\leftrightarrow\mathbf{r}_2\\ \beta_{\mathrm{C}-\mathrm{C}}/\beta=e^{-\eta}, & \text{if } \mathbf{r}_1=\mathbf{r}_{\beta_l},\ \mathbf{r}_2=\mathbf{r}_{\beta_r};\ \mathbf{r}_1\leftrightarrow\mathbf{r}_2\\ \beta_{\mathrm{C}_{\alpha_l}-\mathrm{C}_{\alpha_r}}/\beta\equiv\gamma, & \text{if } \mathbf{r}_1=\mathbf{r}_{\alpha_l},\ \mathbf{r}_2=\mathbf{r}_{\alpha_r};\ \mathbf{r}_1\leftrightarrow\mathbf{r}_2\\ 0, & \text{otherwise,}\end{cases}$$

$$V_{n_{\mathbf{r}_1},n'_{\mathbf{r}_2}}=\beta\begin{cases}\beta_{\mathrm{C}_\alpha-\mathrm{C}_{\alpha'}}/\beta\equiv\gamma_{\mathrm{int}}, & \text{if } n'=n+1(n\neq N),\ \mathbf{r}_1=\mathbf{r}_{\alpha_r},\ \mathbf{r}_2=\mathbf{r}_{\alpha_l};\\ & \quad n'=n-1(n\neq 1),\ \mathbf{r}_1=\mathbf{r}_{\alpha_l},\ \mathbf{r}_2=\mathbf{r}_{\alpha_r};\\ 0, & \text{otherwise,}\end{cases}\tag{2}$$

where ϵ_X is the difference in Coulomb integrals between heteroatom X and carbon C expressed in units of β—the resonance integral in the undimerized carbon backbone, i.e., in a carbon chain with zero alternation parameter $\eta=0$ [in commonly used notations $\epsilon_X=(\alpha_X-\alpha_{\mathrm{C}})/\beta$]; γ_X, e^{η}, and $e^{-\eta}$ are the resonance integrals (in same units) associated with $X-\mathrm{C}$, double C=C, and single C–C bonds within rings, respectively, while parameter γ_{int} accounts for the difference between the resonance carbon–carbon interaction between and within rings (for a nonperturbed dimerized carbon chain of polyacetylene $\gamma_{\mathrm{int}}=e^{-\eta}$); an additional resonance interaction between alpha carbons within rings[16] is described by parameter γ.

It is convenient to formulate the eigenvalue-eigenstate problem in terms of the (dimensionless) monomer Green function

$$G^M(E)=\frac{\gamma_{\mathrm{int}}}{E-\beta^{-1}H^M},\tag{3}$$

where E is the π electron energy in units β.

Substituting the expansion of molecular orbitals (MO) over atomic orbitals

$$\Psi=\sum_n\sum_{\mathbf{r}}\psi_{n_{\mathbf{r}}}|n_{\mathbf{r}}\rangle\tag{4}$$

into the Schrödinger equation with Hamiltonian (1) and using the method of Lifshits[28] and Koster and Slater,[29] one easily arrives at the following equation for the MO coefficients

$$\psi_{n_{\mathbf{r}}}=(1-\delta_{n,1})\psi_{(n-1)_{\mathbf{r}_{\alpha_r}}}G^M_{\mathbf{r},\mathbf{r}_{\alpha_l}}(E)+(1-\delta_{n,N})\psi_{(n+1)_{\mathbf{r}_{\alpha_l}}}G^M_{\mathbf{r},\mathbf{r}_{\alpha_r}}(E),\tag{5}$$

where without loss of generality the Hermitian matrix $G^M_{\mathbf{r},\mathbf{r}'}(E)=\langle n_{\mathbf{r}}|G^M(E)|n_{\mathbf{r}'}\rangle$ is supposed to be real.

Note that passing from $H_{n_{\mathbf{r}_1},n'_{\mathbf{r}_2}}\psi_{n'_{\mathbf{r}_2}}=E\psi_{n_{\mathbf{r}_1}}$ to (5) is very useful since the latter equation corresponds to the one-dimensional problem with nearest-neighbor interaction which is known to have the exact solution.

The above set of equations is completely equivalent to the initial Schrödinger problem but special care should be taken, if a π electron wave function has nodes at all binding sites, i.e., at carbons in α position, $\psi_{n_{\mathbf{r}_{\alpha_l}}}=\psi_{n_{\mathbf{r}_{\alpha_r}}}=0$. Obviously, such states are not affected by the resonance interaction between monomers. Therefore, being N-fold degenerate oligomer states, they are the subject to the solution of a much more simple problem for an isolated monomer that has to be solved separately (see below).

To meet the boundary condition for the free-end chain model of oligomers

$$\psi_{0_{\mathbf{r}_{\alpha_r}}}=\psi_{(N+1)_{\mathbf{r}_{\alpha_l}}}=0,\tag{6}$$

we set

$$\psi_{n_{\mathbf{r}_{\alpha_r}}}=A\sin(\xi n),\quad \psi_{n_{\mathbf{r}_{\alpha_l}}}=B\sin[\xi(N+1-n)].\tag{7}$$

These expressions satisfy Eq. (5) with $n=1$, $\mathbf{r}=\mathbf{r}_{\alpha_l}$ and $n=N$, $\mathbf{r}=\mathbf{r}_{\alpha_r}$, if

$$\frac{\sin(N\xi)}{\sin[(N-1)\xi]}=G^M_{\mathbf{r}_{\alpha_l},\mathbf{r}_{\alpha_r}}(E).\tag{8}$$

The rest of the equations of set (5) at $\mathbf{r}=\mathbf{r}_{\alpha_{l,r}}$ are also satisfied if additionally,

$$B/A=\frac{\sin\xi}{\sin[\xi(N-1)]G^M_{\mathbf{r}_{\alpha_r},\mathbf{r}_{\alpha_r}}(E)}=\frac{\sin[\xi(N-1)]G^M_{\mathbf{r}_{\alpha_l},\mathbf{r}_{\alpha_l}}(E)}{\sin\xi}.\tag{9}$$

Thus, the eigenvalue problem

$$\mathrm{Det}|\beta^{-1}H_{n_{\mathbf{r}_1},n'_{\mathbf{r}_2}}-\delta_{\mathbf{r}_1,\mathbf{r}_2}\delta_{n,n'}E|=0\tag{10}$$

is reduced to a set of two transcendent equations, namely, Eq. (8) and

$$\frac{\sin^2\xi}{\sin^2[\xi(N-1)]}=G^M_{\mathbf{r}_{\alpha_r},\mathbf{r}_{\alpha_r}}(E)G^M_{\mathbf{r}_{\alpha_l},\mathbf{r}_{\alpha_l}}(E),\tag{11}$$

which with account to (8) can be rewritten as

$$\cos\,\xi=\frac{1}{2G^M_{\mathbf{r}_{\alpha_l},\mathbf{r}_{\alpha_r}}(E)}\{1-G^M_{\mathbf{r}_{\alpha_l},\mathbf{r}_{\alpha_l}}(E)G^M_{\mathbf{r}_{\alpha_r},\mathbf{r}_{\alpha_r}}(E)+[G^M_{\mathbf{r}_{\alpha_l},\mathbf{r}_{\alpha_r}}(E)]^2\}. \tag{12}$$

Note that the order of secular equation (10) can be reduced in a similar way by using the transfer matrix[30] and polynomial matrix[31] methods.

In the case of the periodic boundary conditions Eq. (12) remains valid but we do not need an additional equation (8) for determining the quantum number ξ which acquires its usual meaning of the quasi-impulse $\xi=ka=(2\pi/N)j$, $j=0,1,...,N-1$, where a is the distance between monomers.

Equations (5), (7)–(9), and (12) give the full description of one-electron properties of linear conjugated molecules of the type $M-M-\cdots-M$. To find solutions to these equations one needs to specify the monomer Green function. However, certain conclusions concerning the π electronic structure of conjugated polymers can be made by using general properties of $G^M(E)$.

A. Band spectrum

The Green function matrix elements $G^M_{\mathbf{r}_{\alpha_l},\mathbf{r}_{\alpha_l}}(E)$, $G^M_{\mathbf{r}_{\alpha_r},\mathbf{r}_{\alpha_r}}(E)$, and $G^M_{\mathbf{r}_{\alpha_l},\mathbf{r}_{\alpha_r}}(E)$ which appeared in Eqs. (8) and (12) can be represented as rational functions of the type $P'_{N'_M}(E)/P_{N_M}(E)$, where P and P' are polynomials of the N_Mth and N'_Mth and ($N'_M<N_M$) degree, respectively, and N_M is equal to or less than the number of π electron levels of the monomer. (The latter case is realized when some of the monomer π electron states have nodes at alpha carbons.) Thus, at any value of ξ, $0\leqslant\xi\leqslant\pi$, and independently of the oligomer length, Eq. (12) is nothing more than a polynomial of the N_Mth degree which has N_M real solutions $E_\mu(\xi_\mu)$, $\mu=1,2,...,N_M$, determining π electron bands of the molecule. For each band Eq. (8) with E replaced by $E_\mu(\xi_\mu)$ determines N values of ξ. An example of graphical solution of Eq. (12) is shown in Fig. 3.

One can see an obvious advantage of Eqs. (8) and (12) in comparison with the initial eigenvalue problem (10). This is the reduction of the order of the secular equation to solve from $N\times N_M$ to N_M. Furthermore, the obtained form of secular equation in terms of the monomer Green function makes apparent some peculiar features of the π electronic structure that fall into focus below.

B. Discrete levels and band joining

It will be shown below that not all solutions to Eq. (8) are necessarily real. There also can be imaginary solutions with $\xi=i\delta$, $\xi=\pi+i\delta'$. As seen from Fig. 3, the energies of such states are outside the π electron bands, so that even in the infinite chain limit they correspond to discrete levels in the spectrum. The amplitudes of MO coefficients (7) with imaginary value of ξ decrease with the increase of distance from the chain ends, i.e., the π electron tends to reside near the chain ends. The electron localization effect is more pronounced in longer chains but it can also be quite substantial in oligomers of intermediate length.

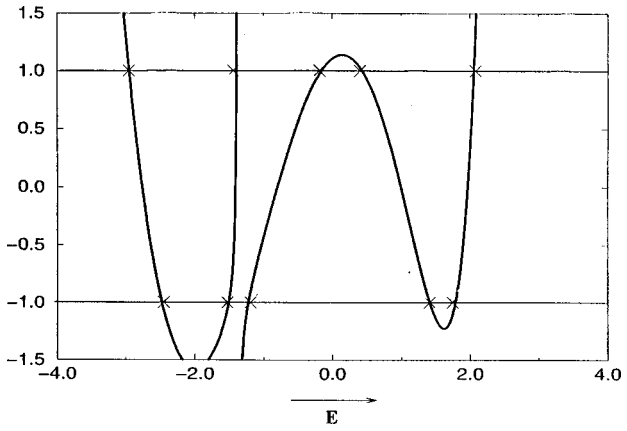

FIG. 3. Graphic solution of Eq. (12) in the case of heterocyclic polymer. The monomer Green function matrix elements [defined in Eq. (24)] are calculated with Hückel parameters suggested for furan (see Ref. 43): $\epsilon_X=2.0$, $\gamma_X=0.8$, and the difference between double and single carbon—carbon bonds is assumed to correspond $\eta=0.1$. Solid curves represent the right-hand side of (12) as a function of energy (in units $|\beta|$). The solutions correspond to intersections of horizontal lines within interval $\{-1,1\}$ with solid lines within π band intervals between the band-edge energies: (from left to right) E_{1_-},E_{1_+}; E_{2_-},E_{X_-}; E_{X_+},E_{2_+}; E_{3_-},E_{4_-}; and E_{3_+},E_{4_+}. The band-edge energies $E_{i_\pm}$ $(i=1,2,3,4)$ $E_{X_\pm}$ are indicated by crosses; the analytical definition of these quantities is given in Sec III B1.

It is worth emphasizing that these kinds of local states known in literature as Tamm/Shockley states[32] are usually associated with the end defects and have been extensively studied in end-substituted polyenes.[33–38] As it will be shown later, the presence of discrete (local) levels in the π electron spectrum of heterocyclic oligomers/polymers is very likely even without the perturbation of the chain ends.

Now consider the limit $N\to\infty$. In this case, the local state spectrum of the polymer is determined by solutions to the equation

$$G^M_{\mathbf{r}_{\alpha_l},\mathbf{r}_{\alpha_l}}(E)G^M_{\mathbf{r}_{\alpha_r},\mathbf{r}_{\alpha_r}}(E)=0, \tag{13}$$

which for $\xi=i\delta$ and $\xi=\pi+i\delta'$ follow directly from Eqs. (8) and (12).

Remarkably, zeros (not poles) of the monomer Green function components give the physically sound quantities. These are discrete level energies in the polymer spectrum henceforth denoted as $E^{(i)}_{\mathrm{loc}}$. The corresponding values of δ and δ' can easily be found from Eq. (8)

$$\delta^{(i)}_{\mathrm{loc}}=\ln|G^M_{\mathbf{r}_{\alpha_l},\mathbf{r}_{\alpha_r}}(E^{(i)}_{\mathrm{loc}})|,$$
$$\text{if } E_{\mathrm{top}}(\xi=0)<E^{(i)}_{\mathrm{loc}}<E_{\mathrm{bottom}}(\xi=0),$$
$$\delta'^{(i)}_{\mathrm{loc}}=\ln|G^M_{\mathbf{r}_{\alpha_l},\mathbf{r}_{\alpha_r}}(E^{(i)}_{\mathrm{loc}})|,$$
$$\text{if } E_{\mathrm{top}}(\xi=\pi)<E^{(i)}_{\mathrm{loc}}<E_{\mathrm{bottom}}(\xi=\pi), \tag{14}$$

where it is indicated which gap refers to the discrete level: between the adjacent band edges which correspond to $\xi=0$ or $\xi=\pi$.

Thus, according to (13), at energies of local states at least one diagonal component of the monomer Green function, which refers to binding sites, is equal to zero, and

$$|G^M_{\mathbf{r}_{\alpha_l},\mathbf{r}_{\alpha_r}}(E^{(i)}_{\rm loc})|>1. \tag{15}$$

If for some of the solutions to Eq. (13)

$$|G^M_{\mathbf{r}_{\alpha_l},\mathbf{r}_{\alpha_r}}(E)|=1 \tag{16}$$

[and thus, in the limit $N\to\infty$, Eq. (8) is satisfied at $\xi=0,\pi$] we have the case of joining bands, i.e., closing of the corresponding gap. Such solutions have the meaning of band-edge energies.

Obviously, in the energy interval, which corresponds to any of forbidden zones, each of diagonal Green function components $G^M_{\mathbf{r}_{\alpha_l},\mathbf{r}_{\alpha_l}}(E)$ and $G^M_{\mathbf{r}_{\alpha_r},\mathbf{r}_{\alpha_r}}(E)$ is equal to zero at only one particular energy. Therefore, in polymers consisting of monomers such that $G^M_{\mathbf{r}_{\alpha_l},\mathbf{r}_{\alpha_l}}(E)=G^M_{\mathbf{r}_{\alpha_r},\mathbf{r}_{\alpha_r}}(E)$, as is the case of heterocyclic polymers, the gap closing occurs if at the indicated energy Eq. (16) is fulfilled. It also follows from Eq. (13) that the local states in this kind of conducting polymer must be doubly degenerate, that is they are coupled genetically with two bands.

C. Band degeneracy

For some monomers, including five-membered heterocycles, the nondiagonal Green function component $G^M_{\mathbf{r}_{\alpha_l},\mathbf{r}_{\alpha_r}}(E)$ can be equal to zero at certain values of energy, hereinafter denoted as $E^{(i)}_{\rm deg}$, which satisfy the equation

$$G^M_{\mathbf{r}_{\alpha_l},\mathbf{r}_{\alpha_r}}(E)=0. \tag{17}$$

As seen from Eq. (12), these energies represent a special case that has to be considered separately. In particular, for the right-hand side of (12) be finite at solutions to (17) the following relation must hold

$$G^M_{\mathbf{r}_{\alpha_l},\mathbf{r}_{\alpha_l}}(E^{(i)}_{\rm deg})G^M_{\mathbf{r}_{\alpha_r},\mathbf{r}_{\alpha_r}}(E^{(i)}_{\rm deg})=1. \tag{18}$$

Note that Eqs. (17) and (18) are equivalent to the condition of the coincidence of top and bottom of one and the same band. This means that if both these equations hold Eq. (12), taken at $\xi=0$ and $\xi=\pi$, is satisfied at one and the same value of energy.

If the condition just mentioned is fulfilled, the wave function amplitudes (5) referred to the binding sites are determined by

$$\begin{aligned}\psi_{n_{\mathbf{r}_{\alpha_l}}}&=(1-\delta_{n,1})\psi_{(n-1)_{\mathbf{r}_{\alpha_r}}}G^M_{\mathbf{r}_{\alpha_l},\mathbf{r}_{\alpha_l}}(E^{(i)}_{\rm deg}),\\ \psi_{n_{\mathbf{r}_{\alpha_r}}}&=(1-\delta_{n,N})\psi_{(n+1)_{\mathbf{r}_{\alpha_l}}}G^M_{\mathbf{r}_{\alpha_r},\mathbf{r}_{\alpha_r}}(E^{(i)}_{\rm deg}).\end{aligned} \tag{19}$$

All nontrivial solutions of the above set of equations supplemented by Eq. (5) for $\mathbf{r}\neq\mathbf{r}_{\alpha_l},\mathbf{r}_{\alpha_r}$ can be represented as linear combinations of π electron states confined within all possible pairs of adjacent monomers for which MO coefficients related to binding sites are determined as

$$\begin{aligned}\psi_{n_{\mathbf{r}_{\alpha_r}}}&=\text{const}\cdot\delta_{n,n'},\\ \psi_{n_{\mathbf{r}_{\alpha_l}}}&=\text{const}\cdot\delta_{n,(n'+1)}G^M_{\mathbf{r}_{\alpha_l},\mathbf{r}_{\alpha_l}}(E^{(i)}_{\rm deg}),\end{aligned} \tag{20}$$

where $n'=1,2,...,N-1$. Thus, zeros of the nondiagonal matrix element $G^M_{\mathbf{r}_{\alpha_l},\mathbf{r}_{\alpha_r}}(E)$ correspond to $(N-1)$-fold degenerate bands in a polymer consisting of monomers M.

Up to this point, the particular structure of the heterocycle ring has not been used. Therefore, all relations obtained above, as well as the conclusions made, are valid for arbitrary conjugated oligomer/polymer whose chemical structure is covered by formula $M-M-\cdots-M$. In Sec. III, we specify the above results for heterocyclic oligomers and polymers.

III. π ELECTRONIC STRUCTURE OF HETEROCYCLIC OLIGOMERS

A. Green function of heterocycle

The monomer Green function is the basic quantity in the present formalism which has been shown to be closely interrelated with the oligomer/polymer π electronic structure. Therefore, we start our discussion of heterocyclic polymers with derivation of the Green function for five-membered heterocycles.

At first, in order not to overload the model by parameters, we ignore the contribution coming from the direct interaction between alpha carbons within rings described by parameter γ. (The inclusion of this interaction is straightforward and considered below.) Then, the solution of the eigenvalue-eigenstate problem with the monomer Hamiltonian H^M defined in Eq. (2) with $\gamma=0$ can be represented as

$$\begin{aligned}&\text{Det}|H^M_{\mathbf{r}_1,\mathbf{r}_2}-\delta_{\mathbf{r}_1,\mathbf{r}_2}E|\\ &\equiv\mathscr{D}=(E^2+Ee^{-\eta}-e^{2\eta})[(E-\epsilon_X)\\ &\qquad\times(E^2-Ee^{-\eta}-e^{2\eta})-2\gamma_X^2(E-e^{-\eta})]=0,\end{aligned} \tag{21}$$

the secular equation, and $\Psi^M=\Sigma_{\mathbf{r}}\psi^M_{\mathbf{r}}|\mathbf{r}\rangle$ the molecular orbitals, where

$$\psi^M_{\mathbf{r}}=\left[2\left(1+\frac{e^{2\eta}}{(E+e^{-\eta})^2}\right)\right]^{-1/2}\begin{cases}-1, & \mathbf{r}=\mathbf{r}_{\alpha_l},\\ 1, & \mathbf{r}=\mathbf{r}_{\alpha_r},\\ -\dfrac{e^{\eta}}{E+e^{-\eta}}, & \mathbf{r}=\mathbf{r}_{\beta_l},\\ \dfrac{e^{\eta}}{E+e^{-\eta}}, & \mathbf{r}=\mathbf{r}_{\beta_r},\\ 0, & \mathbf{r}=\mathbf{r}_X,\end{cases} \tag{22}$$

if E is a solution to $E^2+Ee^{-\eta}-e^{2\eta}=0$; and

$$\psi_{\mathbf{r}}^{M}=\left[2\left(1+\frac{e^{2\eta}}{(E-e^{-\eta})^2}+\frac{2\gamma_X^2}{(E-\epsilon_X)^2}\right)\right]^{-1/2}\begin{cases}1, & \mathbf{r}=\mathbf{r}_{\alpha_r}, \quad \mathbf{r}=\mathbf{r}_{\alpha_l},\\ \dfrac{e^{\eta}}{E-e^{-\eta}}, & \mathbf{r}=\mathbf{r}_{\beta_r}, \quad \mathbf{r}=\mathbf{r}_{\beta_l},\\ \dfrac{2\gamma_X}{E-\epsilon_X}, & \mathbf{r}=\mathbf{r}_X,\end{cases} \tag{23}$$

if E is a solution to $(E-\epsilon_X)(E^2-Ee^{-\eta}-e^{2\eta})-2\gamma_X^2(E-e^{-\eta})=0$.

Thus, the monomer Green function takes the form

$$G^{M}_{\mathbf{r}_1,\mathbf{r}_2}(E)=\frac{\gamma_{\mathrm{int}}}{\mathscr{D}}\begin{cases}E(E-\epsilon_X)[E^2-2\cosh(2\eta)]-\gamma_X^2(E^2-e^{-2\eta}), & \mathbf{r}_1=\mathbf{r}_2=\mathbf{r}_{\alpha_{l,r}},\\ E(E-\epsilon_X)(E^2-e^{2\eta})-\gamma_X^2(2E^2-e^{2\eta}) & \mathbf{r}_1=\mathbf{r}_2=\mathbf{r}_{\beta_{l,r}},\\ E^2[E^2-2\cosh(2\eta)]-e^{2\eta}(E^2-e^{2\eta}), & \mathbf{r}_1=\mathbf{r}_2=\mathbf{r}_X,\\ e^{\eta}(E-\epsilon_X)+\gamma_X^2(E^2-e^{-2\eta}), & \mathbf{r}_1=\mathbf{r}_{\alpha_l}, \quad \mathbf{r}_2=\mathbf{r}_{\alpha_r},\\ E^2(E-\epsilon_X)-\gamma_X^2(e^{2\eta}-2Ee^{-\eta}), & \mathbf{r}_1=\mathbf{r}_{\beta_l}, \quad \mathbf{r}_2=\mathbf{r}_{\beta_r},\\ e^{\eta}[(E-\epsilon_X)(E^2-e^{-2\eta})-\gamma_X^2(E-e^{-\eta})], & \mathbf{r}_1=\mathbf{r}_{\alpha_{l(r)}}, \quad \mathbf{r}_2=\mathbf{r}_{\beta_{l(r)}},\\ E(E-\epsilon_X)+\gamma_X^2e^{\eta}(E-e^{-\eta}), & \mathbf{r}_1=\mathbf{r}_{\alpha_{l(r)}}, \quad \mathbf{r}_2=\mathbf{r}_{\beta_{r(l)}},\\ \gamma_X(E-e^{-\eta})(E^2+Ee^{-\eta}-e^{2\eta}), & \mathbf{r}_1=\mathbf{r}_X, \quad \mathbf{r}_2=\mathbf{r}_{\alpha_{l,r}},\\ \gamma_X[e^{\eta}(E^2-e^{2\eta})+E], & \mathbf{r}_1=\mathbf{r}_X, \quad \mathbf{r}_2=\mathbf{r}_{\beta_{l,r}}.\end{cases} \tag{24}$$

Introducing the numbering of the five-membered ring levels such that

$$\lim_{\gamma_X\to 0}E_i^M=E_i^M|_{\gamma_X=0}, \quad i=1,2,3,4,X, \tag{25}$$

the explicit expressions of solutions to Eq. (21) can be represented as

$$E_{1,3}^M=-2\sqrt{\frac{p}{3}}\cos\frac{\alpha\pm\pi}{3}+\frac{e^{-\eta}+\epsilon_X}{3},$$

$$\lim_{\gamma_X\to 0}E_{1,3}^M=E_{1,3}^M\Big|_{\gamma_X=0}=\frac{e^{-\eta}}{2}\pm\sqrt{\frac{e^{-2\eta}}{4}+e^{2\eta}},$$

$$E_{2,4}^M=E_{2,4}^M|_{\gamma_X=0}=-\frac{e^{-\eta}}{2}\pm\sqrt{\frac{e^{-2\eta}}{4}+e^{2\eta}},$$

$$E_X^M=2\sqrt{\frac{p}{3}}\cos\frac{\alpha}{3}+\frac{e^{-\eta}+\epsilon_X}{3},$$

$$\lim_{\gamma_X\to 0}E_X^M=E_X^M\Big|_{\gamma_X=0}=\epsilon_X, \tag{26}$$

where we use the following abbreviation

$$\cos\alpha=-\frac{q}{2\sqrt{\left(\frac{p}{3}\right)^3}}, \tag{27}$$

and

$$p=\tfrac{1}{3}[e^{-2\eta}+\epsilon_X(\epsilon_X-e^{-\eta})]+e^{2\eta}+2\gamma_X^2,$$

$$q=\tfrac{1}{3}[e^{2\eta}(2\epsilon_X-e^{-\eta})-2\gamma_X^2(\epsilon_X-2e^{-\eta})-\tfrac{1}{9}(\epsilon_X+e^{-\eta})\times(\epsilon_X-2e^{-\eta})(2\epsilon_X-e^{-\eta})]. \tag{28}$$

It is seen that two of five monomer π electron states do not depend on the heteroatom parameters. These are levels which correspond to antisymmetric states of four-carbon segment C=C–C=C—the elementary cell of *cis*-polyacetylene chain.

Note also that at the particular value of heteroatom site energy $\epsilon_X=e^{-\eta}$ the order of the nominator and denominator of the Green function matrix elements, which enter the set of secular equations (8) and (12), is reduced by unity. This is just the case when in one of the monomer eigenstates, namely, with the energy $E=\epsilon_X=e^{-\eta}$, the π electron density at alpha carbons (binding sites) is equal to zero. In oligomer/polymer this level is not split into a band.

B. Band spectrum

Taking into account explicit expressions (24) of Green function components $G^{M}_{\mathbf{r}_{\alpha_l},\mathbf{r}_{\alpha_l}}(E)=G^{M}_{\mathbf{r}_{\alpha_r},\mathbf{r}_{\alpha_r}}(E)$ and $G^{M}_{\mathbf{r}_{\alpha_l},\mathbf{r}_{\alpha_r}}(E)$, and the relation

$$[G^{M}_{\mathbf{r}_{\alpha_l},\mathbf{r}_{\alpha_l}}(E)]^2-[G^{M}_{\mathbf{r}_{\alpha_l},\mathbf{r}_{\alpha_r}}(E)]^2=\frac{\gamma_{\mathrm{int}}^2}{\mathscr{D}}(E-\epsilon_X)(E^2-e^{-2\eta}), \tag{29}$$

Eq. (12) can be rewritten in the form

$$\begin{aligned}2\gamma_{\mathrm{int}}[e^{\eta}(E-\epsilon_X)+\gamma_X^2(E^2-e^{-2\eta})]\cos\xi&=(E-\epsilon_X)[(E^2-e^{2\eta})^2-E^2e^{-2\eta}-\gamma_{\mathrm{int}}^2(E^2-e^{-2\eta})]\\&\quad-2\gamma_X^2(E-e^{-\eta})(E^2+Ee^{-\eta}-e^{2\eta}).\end{aligned} \tag{30}$$

As it was pointed out above, for the periodic chain model the solutions to this equation determine the dispersion relations $E_{\mu}[\xi=(2\pi/N)j]$ for five π electron bands of heterocyclic chain oligomers/polymers. For the determination of

the π electron spectrum of terminated chain consisting of heterocyclic rings Eq. (30) has to be supplemented by Eq. (8) with $G^M_{\mathbf{r}_{\alpha_l},\mathbf{r}_{\alpha_r}}(E)$ defined in (24).

Under the assumption that the C–C bond alternation of parent carbon chain is not affected by heteroatoms, $\gamma_{\rm int} = \exp(-\eta)$, Eq. (30) simplifies and takes the form

$$2[(E-\epsilon_X)+\gamma_X^2 e^{-\eta}(E^2-e^{-2\eta})]\cos\xi = (E-\epsilon_X)\{[E^2-2\cosh(2\eta)]^2-2\}-2\gamma_X^2(E-e^{-\eta}) \times(E^2+Ee^{-\eta}-e^{2\eta}). \quad (31)$$

$$E^2(\xi)|_{\gamma_X=0}=\left|e^{2\eta}+\frac{e^{-2\eta}+\gamma_{\rm int}^2}{2}\pm\frac{1}{2}\sqrt{(\gamma_{\rm int}^2-e^{-2\eta})^2+4(1+\gamma_{\rm int}^2e^{2\eta}+2\gamma_{\rm int}e^{\eta}\cos\xi)}\right|. \quad (32)$$

By setting in Eq. (32) the intermonomer interaction equal to $\gamma_{\rm int}=\exp(-\eta)$, one arrives at

$$E(\xi)|_{\gamma_X=0}=\pm\sqrt{2\left(\cosh(2\eta)\pm\cos\frac{\xi}{2}\right)}, \quad (33)$$

which is immediately recognized as the handbook polyene/polyacetylene spectrum in the Hückel approximation.

1. Band-edge energies

A remarkable property of Eq. (30) is that, unlike the case of arbitrary values of ξ, the energies of band edges, which are approached by the band-edge states as $N\to\infty$ and where $\xi=0$ or π, can be divided on those which are affected and not affected by the X–C resonance interaction. Indeed, for $\xi=0$ we have from (12)

$$G^M_{\mathbf{r}_{\alpha_l},\mathbf{r}_{\alpha_r}}(E)\pm G^M_{\mathbf{r}_{\alpha_l},\mathbf{r}_{\alpha_l}}(E)=1, \quad (34)$$

and similarly, for $\xi=\pi$

$$G^M_{\mathbf{r}_{\alpha_l},\mathbf{r}_{\alpha_r}}(E)\pm G^M_{\mathbf{r}_{\alpha_l},\mathbf{r}_{\alpha_l}}(E)=-1. \quad (35)$$

Thus, the band-edge energies are determined by the following set of equations:

$$E^2+(e^{-\eta}-\gamma_{\rm int})E-\gamma_{\rm int}\,e^{-\eta}-e^{2\eta}=0,$$

$$E_{2_+(4_+)}=-\frac{e^{-\eta}-\gamma_{\rm int}}{2}+(-)\sqrt{\frac{(e^{-\eta}+\gamma_{\rm int})^2}{4}+e^{2\eta}}\quad(\xi=\pi), \quad (36)$$

$$E^2+(e^{-\eta}+\gamma_{\rm int})E+\gamma_{\rm int}\,e^{-\eta}-e^{2\eta}=0,$$

Note that unlike the monomer levels, the oligomer/polymer bands cannot be divided on those affected by heteroatoms and those which are not, including the case of N-fold degenerate X band, i.e., when $\epsilon_X=\exp(-\eta)$ and the order of equations (30), (31) is reduced by unity.

In the case of zero X–C interaction, $\gamma_X=0$, apart of a trivial solution which corresponds to isolated levels of X atoms, $E=\epsilon_X$, Eq. (30) describes four π electron bands of the nonperturbed carbon chain of *cis*-polyene/polyacetylene with arbitrary interaction between monomers. The solutions to this equation are

$$E_{2_-(4_-)}=-\frac{e^{-\eta}+\gamma_{\rm int}}{2}+(-)\sqrt{\frac{(e^{-\eta}-\gamma_{\rm int})^2}{4}+e^{2\eta}}\quad(\xi=0), \quad (37)$$

$$(E-\epsilon_X)[E^2-(e^{-\eta}+\gamma_{\rm int})E+\gamma_{\rm int}\,e^{-\eta}-e^{2\eta}] -2\gamma_X^2(E-e^{-\eta})=0\quad(\xi=0), \quad (38)$$

$$(E-\epsilon_X)[E^2-(e^{-\eta}-\gamma_{\rm int})E-\gamma_{\rm int}\,e^{-\eta}-e^{2\eta}] -2\gamma_X^2(E-e^{-\eta})=0\quad(\xi=\pi), \quad (39)$$

where the integer of the subscript in the accepted notations refers to the corresponding monomer level to which the given solution is connected genetically (i.e., $\lim_{\gamma_{\rm int}\to0}E_{i\pm}\to E_i^M$), whereas the sign in subscript refers to the upper (+) and lower (−) edge of the band in the same limit.

To avoid confusion, it is worth stressing that numbering in notations of the band-edge energies may have nothing in common with their sequence in the energy scale. The latter depends on the heteroatom parameters and also on $\gamma_{\rm int}$ and thus, it cannot be reflected in notations without fixing these parameters.

In the particular case of degenerate X band, $\epsilon_X=\exp(-\eta)$, solutions of Eqs. (38) and (39) take an especially simple form

$$E_{1_+(3_+)}=\frac{e^{-\eta}+\gamma_{\rm int}}{2}+(-)\sqrt{\frac{(e^{-\eta}-\gamma_{\rm int})^2}{4}+e^{2\eta}+2\gamma_X^2},$$

$$E_{X_+}=\epsilon_X=e^{-\eta},$$

$$E_{1_-(3_-)}=\frac{e^{-\eta}-\gamma_{\rm int}}{2}+(-)\sqrt{\frac{(e^{-\eta}+\gamma_{\rm int})^2}{4}+e^{2\eta}+2\gamma_X^2},$$
$$E_{X_-}=\epsilon_X=e^{-\eta} \tag{40}$$

making apparent the dependence of the band structure on the characteristic parameters.

2. Edge states

Now consider MO coefficients at X atoms which according to the results of Sec. II can be represented as

$$\psi_{n_{\mathbf{r}_X}}=\text{const}\cdot\frac{G^M_{\mathbf{r}_{\alpha_l},\mathbf{r}_X}(E)}{G^M_{\mathbf{r}_{\alpha_l},\mathbf{r}_{\alpha_l}}(E)}\{\sin(n\xi)+[G^M_{\mathbf{r}_{\alpha_l},\mathbf{r}_{\alpha_l}}(E)-G^M_{\mathbf{r}_{\alpha_l},\mathbf{r}_{\alpha_r}}(E)]\sin[(n-1)\xi]\}. \tag{41}$$

At the band-edge energies determined by Eqs. (36) and (37) the difference between the diagonal and nondiagonal Green function components, which appeared in (41), is equal to 1 and -1, respectively. Consequently, at these energies $\psi_{n_{\mathbf{r}_X}}=0$. This means that the corresponding frontier orbitals have no contribution from heteroatoms. It is also seen that these states are antisymmetric: $\psi_{n_{\mathbf{r}_{\alpha_l}}}+\psi_{n_{\mathbf{r}_{\alpha_r}}}=\psi_{n_{\mathbf{r}_{\beta_l}}}+\psi_{n_{\mathbf{r}_{\beta_r}}}=0$.

The main conclusion that follows from the above equations is that in heterocyclic polymers there are always four band-edge π electron states which do not depend on parameters of heteroatoms.

C. Local state spectrum

In the case of heterocyclic polymers, Eq. (13), which determines the spectrum of local states, can be written as follows

$$E(E-\epsilon_X)[E^2-2\cosh(2\eta)]-\gamma_X^2(E^2-e^{-2\eta})=0. \tag{42}$$

(To recall, all local states are doubly degenerate.) If neither of the monomer eigenstates has poles at binding sites, i.e., $\epsilon_X\neq\exp(-\eta)$, Eq. (42) has four real solutions which correspond to zeros of $G^M_{\mathbf{r}_{\alpha_l},\mathbf{r}_{\alpha_l}}(E)$ in the energy intervals between monomer levels.

As it was shown above, the solutions to Eq. (42) correspond to discrete levels of the system, if inequality (15) is satisfied, and they determine the energies of band joining, if Eq. (16) is obeyed. In other words, Eqs. (15) and (16) give relations between parameters of the system the fulfillment of which is necessary for the appearance of local states and the band gap closing in the polymer spectrum. With account to explicit expression $G^M_{\mathbf{r}_{\alpha_l},\mathbf{r}_{\alpha_r}}(E)$, these relations take the form

$$\gamma_{\rm int}>\left|E^{(i)}_{\rm loc}-\frac{e^{2\eta}}{E^{(i)}_{\rm loc}+e^{-\eta}}\right|, \tag{43}$$

and

$$\gamma_{\rm int}=\left|E^{(i)}_{\rm loc}-\frac{e^{2\eta}}{E^{(i)}_{\rm loc}+e^{-\eta}}\right|, \tag{44}$$

respectively.

Since the right-hand side of (44) does not depend on $\gamma_{\rm int}$, it is an inherent property of the monomer which determines the particular value of intermonomer interaction at which the ith gap closes at energy $E^{(i)}_{\rm loc}$ and gives rise to discrete state at this same energy.

The analytical solution to Eq. (42) has a simple form only for the unperturbed parent carbon chain, $\gamma_X=0$, in which case (we are not interested in solution $E=\epsilon_X$ that has a trivial meaning)

$$E^{(1,3)}_{\rm loc}|_{\gamma_X=0}=\pm\sqrt{2\cosh(2\eta)}\quad\text{and}\quad E^{(2)}_{\rm loc}|_{\gamma_X=0}=0, \tag{45}$$

and instead of (43) and (44) we get

$$\gamma_{\rm int}\geqslant\exp(-\eta)\equiv\gamma^{(1)}_{\rm int}\quad\text{and}\quad\gamma_{\rm int}\geqslant\exp(3\eta)\equiv\gamma^{(2)}_{\rm int}. \tag{46}$$

Note that if $\epsilon_X=\exp(-\eta)$, Eq. (42) has a solution which corresponds to the energy of degenerate band $E_{X_\pm}=e^{-\eta}$ (see above). This means that the π electron spectrum of such a system can contain no more than three doubly degenerate local levels. The energies of these levels are

$$E^{(1)}_{\rm loc}=2\sqrt{\frac{2\cosh 2\eta+\gamma_X^2}{3}}\cos\frac{\alpha}{3},$$
$$E^{(2,3)}_{\rm loc}=-2\sqrt{\frac{2\cosh 2\eta+\gamma_X^2}{3}}\cos\left(\frac{\alpha}{3}\pm\frac{\pi}{3}\right), \tag{47}$$

where

$$\cos\alpha=\frac{3\sqrt{3}\,\gamma_X^2e^{-\eta}}{2\sqrt{[2\cosh(2\eta)+\gamma_X^2]^3}}. \tag{48}$$

It is also of interest that the particular value of $E_{X_\pm}$ just indicated above coincides with $\gamma^{(1)}_{\rm int}$, which apart of the meaning specified in Eq. (46), represents the asymptomic value of $E^{\rm edge}_{2_+}|_{\gamma_X=0}=E^{\rm edge}_{2_-}{}_{\gamma_X=0}$ in the limit $\gamma_{\rm int}\to\infty$. Other implications of Eqs. (42)–(44) will be the focus of a forthcoming discussion.

D. Degenerate bands

With regard to the explicit expression of $G^M_{\mathbf{r}_{\alpha_l},\mathbf{r}_{\alpha_r}}(E)$ given in (24), Eq. (17) predicts the possibility of the existence of degenerate bands in the π electron spectrum of conjugated polymers consisting of heterocyclic rings at two different energies

$$E^{1,2}_{\rm deg}=-\frac{e^{\eta}}{2\gamma_X^2}[1\pm\sqrt{1+4\gamma_X^2e^{-\eta}(\epsilon_X+\gamma_X^2e^{-3\eta})}], \tag{49}$$

if for these energies Eq. (18) is fulfilled. The substitution of (49) into (18) gives

$$\gamma_{\rm int}=\frac{e^{\eta}}{2\gamma_X^2}\left|1\pm\sqrt{1+4\gamma_X^2e^{-\eta}(\epsilon_X+\gamma_X^2e^{-3\eta})}-\frac{4\gamma_X^4}{1\pm\sqrt{1+4\gamma_X^2e^{-\eta}(\epsilon_X+\gamma_X^2e^{-3\eta})}-2\gamma_X^2e^{-2\eta}}\right|. \tag{50}$$

It can be verified that the same equation follows from Eq. (44) with $E_{\rm loc}^{(i)}$ replaced by $E_{\rm deg}^{1,2}$, that is the latter relation holds in both cases of band joining and band degeneracy.

Equation (50) represents the necessary and sufficient conditions of the existence of two degenerate bands. In the particular case $\epsilon_X=\exp(-\eta)$, they take the form

$$\gamma_{\rm int}=|e^{\eta}(\gamma_X^2-\gamma_X^{-2})-e^{-\eta}| \tag{51}$$

for sign + and

$$\gamma_{\rm int}=\left|e^{-\eta}-\frac{e^{3\eta}}{2}\right| \tag{52}$$

for sign − in Eq. (50).

E. Effects of interring alpha–carbon direct interaction

As is mentioned in the Introduction, the contribution into the fundamental band gap of heterocyclic polymers coming from the direct interaction between alpha carbons within rings can be quite appreciable, up to 20% of the total gap value.[16] Therefore, it is of importance to trace the role of this interaction in the formation of π electron spectrum. The principal results connected with taking into account the parameter γin the monomer Hamiltonian (2) are as follows.

The effect on the band-edge energies can be described as an effective renormalization of intermonomer interaction $\gamma_{\rm int}\rightarrow\gamma_{\rm int}^{\rm eff}$ with $\gamma_{\rm int}^{\rm eff}=\gamma_{\rm int}-\gamma$ for energies determined by Eqs. (36), (39), and $\gamma_{\rm int}^{\rm eff}=\gamma_{\rm int}+\gamma$ for energies determined by Eqs. (37) and (38). This means, in particular, that for a given value of $\gamma_{\rm int}$ the additional interaction described by γ enlarges the fundamental band gap.

The additional interring resonance interaction leads also to changes of intermonomer interaction at which the gap closing occurs, but there are no effect on energies $E_{\rm loc}^{(i)}$, i.e., Eq. (42) remains unchanged.

By contrast, Eq. (49) has to be replaced by a third order equation which determines the energies of degenerate bands. Consequently, in the presence of the additional interaction, there are three possible values of $\gamma_{\rm int}$ at which one of π electron bands can be degenerate.

F. Molecular orbitals

To obtain explicit expressions of molecular orbitals as functions of ξ for a conjugated chain of five-membered heterocyclic rings, it is more convenient to use not the general form of the monomer Green function defined in Eq. (24), but its equivalent representation valid at the eigenvalues of the given oligomer/polymer only, i.e., at the solutions $E_\mu(\xi_\mu)$ to the set of equations (8) and (30).

For $G^M_{\mathbf{r}_{\alpha_l},\mathbf{r}_{\alpha_l}}(E)$ and $G^M_{\mathbf{r}_{\alpha_l},\mathbf{r}_{\alpha_r}}(E)$ such expressions are already defined in Eqs. (8) and (11). The rest of the matrix elements which appeared in (5) can be found by using the nearest-neighbor relations between the monomer Green function components

$$EG^M_{\mathbf{r}_1,\mathbf{r}_2}(E)=\delta_{\mathbf{r}_1,\mathbf{r}_2}+\beta^{-1}\sum_{\mathbf{r}'}H^M_{\mathbf{r}_1,\mathbf{r}'}G^M_{\mathbf{r}',\mathbf{r}_2}(E), \tag{53}$$

where $H^M_{\mathbf{r}_1,\mathbf{r}_2}$ is defined in Eq. (2). This gives ($\gamma=0$, $N\neq1$)

$$\begin{aligned}
G^M_{\mathbf{r}_{\alpha_l},\mathbf{r}_{\beta_l}}[E_\mu(\xi_\mu)]&=\frac{1}{E_\mu^2(\xi_\mu)-e^{-2\eta}}\times\frac{\sin(N\xi_\mu)\pm e^{\eta}E_\mu(\xi_\mu)\sin\,\xi_\mu}{\sin[(N-1)\xi_\mu]},\\
G^M_{\mathbf{r}_{\alpha_l},\mathbf{r}_{\beta_r}}[E_\mu(\xi_\mu)]&=\frac{1}{E_\mu^2(\xi_\mu)-e^{-2\eta}}\times\frac{e^{\eta}E_\mu(\xi_\mu)\sin(N\xi_\mu)\pm\sin\,\xi_\mu}{\sin[(N-1)\xi_\mu]},\\
G^M_{\mathbf{r}_{\alpha_l},\mathbf{r}_X}[E_\mu(\xi_\mu)]&=\frac{\gamma_X}{E_\mu(\xi_\mu)-\epsilon_X}\frac{\sin(N\xi_\mu)\pm\sin\,\xi_\mu}{\sin[(N-1)\xi_\mu]}.
\end{aligned} \tag{54}$$

Combining Eqs. (5), (7)–(9), (11), and (54), after tedious but straightforward algebra one gets

$$\psi_{n_{\mathbf{r}}}=\text{const}\times\begin{cases}\sin(n\xi_\mu), & \mathbf{r}=\mathbf{r}_{\alpha_r},\\ \pm\sin[(N-n+1)\xi_\mu], & \mathbf{r}=\mathbf{r}_{\alpha_l}\\ \dfrac{1}{E_\mu^2(\xi_\mu)-e^{-2\eta}}\{e^{\eta}E_\mu(\xi_\mu)\sin(n\xi_\mu)\pm\sin[(N-n+1)\xi_\mu]\}, & \mathbf{r}=\mathbf{r}_{\beta_r},\\ \dfrac{1}{E_\mu^2(\xi_\mu)-e^{-2\eta}}\{\sin(n\xi_\mu)\pm e^{\eta}E_\mu(\xi_\mu)\sin[(N-n+1)\xi_\mu]\}, & \mathbf{r}=\mathbf{r}_{\beta_e},\\ \dfrac{\gamma_X}{E_\mu(\xi_\mu)-\epsilon_X}\{\sin(n\xi_\mu)\pm\sin[(N-n+1)\xi_\mu]\}, & \mathbf{r}=\mathbf{r}_X.\end{cases} \tag{55}$$

Substituting the above equations in the normalization condition

$$\sum_{n=1}^{N}(|\psi_{n_{\mathbf{r}_{\alpha_l}}}|^2+|\psi_{n_{\mathbf{r}_{\alpha_r}}}|^2+|\psi_{n_{\mathbf{r}_{\beta_l}}}|^2+|\psi_{n_{\mathbf{r}_{\beta_r}}}|^2+|\psi_{n_{\mathbf{r}_X}}|^2)=1, \tag{56}$$

we obtain

$$\begin{aligned}\text{const}^{-2}=&\left(N-\frac{\sin(N\xi_\mu)\cos[(N+1)\xi_\mu]}{\sin\,\xi_\mu}\right)\\&\times\left(1+\frac{\gamma_X^2}{[E_\mu(\xi_\mu)-\epsilon_X]^2}+\frac{1+e^{2\eta}E_\mu^2(\xi_\mu)}{[E_\mu^2(\xi_\mu)-e^{-2\eta}]^2}\right)\\&\pm\left(\frac{\sin(N\xi_\mu)}{\sin\,\xi_\mu}-N\,\cos[(N+1)\xi_\mu]\right)\\&\times\left(\frac{\gamma_X^2}{[E_\mu(\xi_\mu)-\epsilon_X]^2}+\frac{2e^{\eta}E_\mu(\xi_\mu)}{[E_\mu^2(\xi_\mu)-e^{-2\eta}]^2}\right).\end{aligned} \tag{57}$$

It is interesting to note that Eqs. (55) and (57) are also valid for $N=1$, so that in the latter case, these equations represent the monomer orbitals. It is seen that for the lower sign in (57), where $N=1$, which corresponds to energies $E_{2,4}^M$,

$$\text{const}^{-2}=2\,\sin^2\,\xi_\mu\left(1+\frac{e^{2\eta}}{(E_{2,4}^M+e^{-\eta})^2}\right), \tag{58}$$

that is these states have no contribution from X–C interaction in contrast to the states which correspond to energies $E_{1,3,X}^M$ [upper sign in (57)]

$$\begin{aligned}\text{const}^{-2}=&2\,\sin^2\,\xi_\mu\left(1+\frac{e^{2\eta}}{(E_{1,3,X}^M-e^{-\eta})^2}\right.\\&\left.+\frac{2\gamma_X^2}{(E_{1,3,X}^M-\epsilon_X)^2}\right).\end{aligned} \tag{59}$$

The closed expressions of molecular orbitals for heterocyclic oligomers of arbitrary length, which are presented in Eqs. (55) and (57), can have a number of applications.

IV. MODEL NUMERICAL RESULTS AND THEIR DISCUSSION

Ideally, parameters of model Hamiltonian (1) ϵ_X, γ_X, η, γ, γ_{int}, and β should be determined from experimental data for not too short oligomers of different lengths. An appropriate observable for this purpose is, for instance, the frequency of the lowest dipole $\pi\rightarrow\pi^*$ transition which is directly related to HOMO-LUMO gap $\Delta_{H,L}$.

An excellent example of using spectroscopic data for the determination of Hückel parameters of polyenes and end substituted polyenes is given by Kohler.[39] He obtained values of η and β that quantitatively reproduces all of the 1^1B_u state 0-0 energies of polyenes with 3-to-7 double bonds and of a number of dialkyl- and diphenylpolyenes that have been measured in spectroscopic experiments.

The same strategy has been applied to find parameters ϵ_s and γ_s by measuring the 1^1B_u transition frequency in dithienylpolyenes of different lengths under the assumption that quantities η and β, which have been found for the polyene bridge, are not changed in thiophene rings.[40] To our knowledge, this is the only consistent attempt to obtain ''experimental'' values of ϵ_s, γ_s, η, and β from spectroscopic measurements, and we use these data below.

However, the determination of basic parameters of polythiophene (PTh) in the way just outlined does not fit perfectly to the system in focus since one can expect that the alternation parameter in *trans*-polyenes (studied in Refs. 39 and 40) is not the same as in *cis*-conformation. It is also doubtful that parameters ϵ_s and γ_s, which characterize thiophene rings acting as substitutors, coincide exactly with those of polythiophene. Nevertheless, it will be demonstrated that the use of these parameters gives a reasonable estimate of the fundamental gap.

There are different sets of parameters suggested in literature for one and the same heteroatom, in particular, sulfur. Apart from a scheme based on the carbon matrix elements[41] giving $\epsilon_s=0.5$ and $\gamma_s=0.7$ (both parameters are nearly twice larger than those found by Birnbaum *et al.*,[40] $\epsilon_s=0.25$ and $\gamma_s=0.38$), Van-Catledge[42] suggests a very close value of $\gamma_s=0.69$ but more than twice as large as the value of $\epsilon_s=1.11$. Such a spread in parameters makes a comparison of the theory with experimental results quite ambiguous. On the other hand, using different values of heteroatom parameters gives a deeper insight into the regularities of π electronic structure of heterocyclic polymers—the main goal of this presentation. Therefore, calculations of the gross spectrum structure of PTh, i.e., of π bandwidths, gaps, in-gap levels, and their relative position, are performed for all sets of sulfur parameters indicated above. Two additional sets of parameters are used to model polypyrrole (PPy) spectrum—one with ''standard'' Hückel parameters for NH,[42] $\epsilon_{\text{NH}}=1.5$ and $\gamma_{\text{NH}}=0.8$, and another suggested by Lee and Kertesz:[10] $\epsilon_{\text{NH}}=1.37$, $\gamma_{\text{NH}}=1.27$. And finally following Streitwieser,[43] we assume for polyfuran (PFu) that $\epsilon_0=2.0$, $\gamma_0=0.8$. Just as in the preceding analytical analysis, in all calculations presented below the direct resonance interaction between alpha carbons within rings (parameter γ) is disregarded.

To reduce the number of unknowns, all energies are scaled to $|\beta|$. This implies that quantities $E_{i_\pm}$, $E_{X_\pm}$, E_i^M, and E_X^M [determined by Eqs. (36)–(39) and represented in Figs. 4–6 by solid curves] are taken with negative sign. To exclude the necessity of choice of γ_{int}, the gross spectrum structure is calculated as a function of intermonomer interaction. This dependence has to be understood since in real polymers the value of γ_{int} is influenced by solvent, polymer morphology, and other factors. The presentation of the development of polymer spectrum from monomer levels is also helpful from the methodological point of view making visible the role of intermonomer interaction in the manifestation of heteroatom effects.

It seems reasonable to fix parameter $|\eta|$ at value 0.1 which corresponds to the difference between single and double C–C bonds ≈ 0.1 Å. In order to illustrate the dependence of π electronic structure on the character of backbone

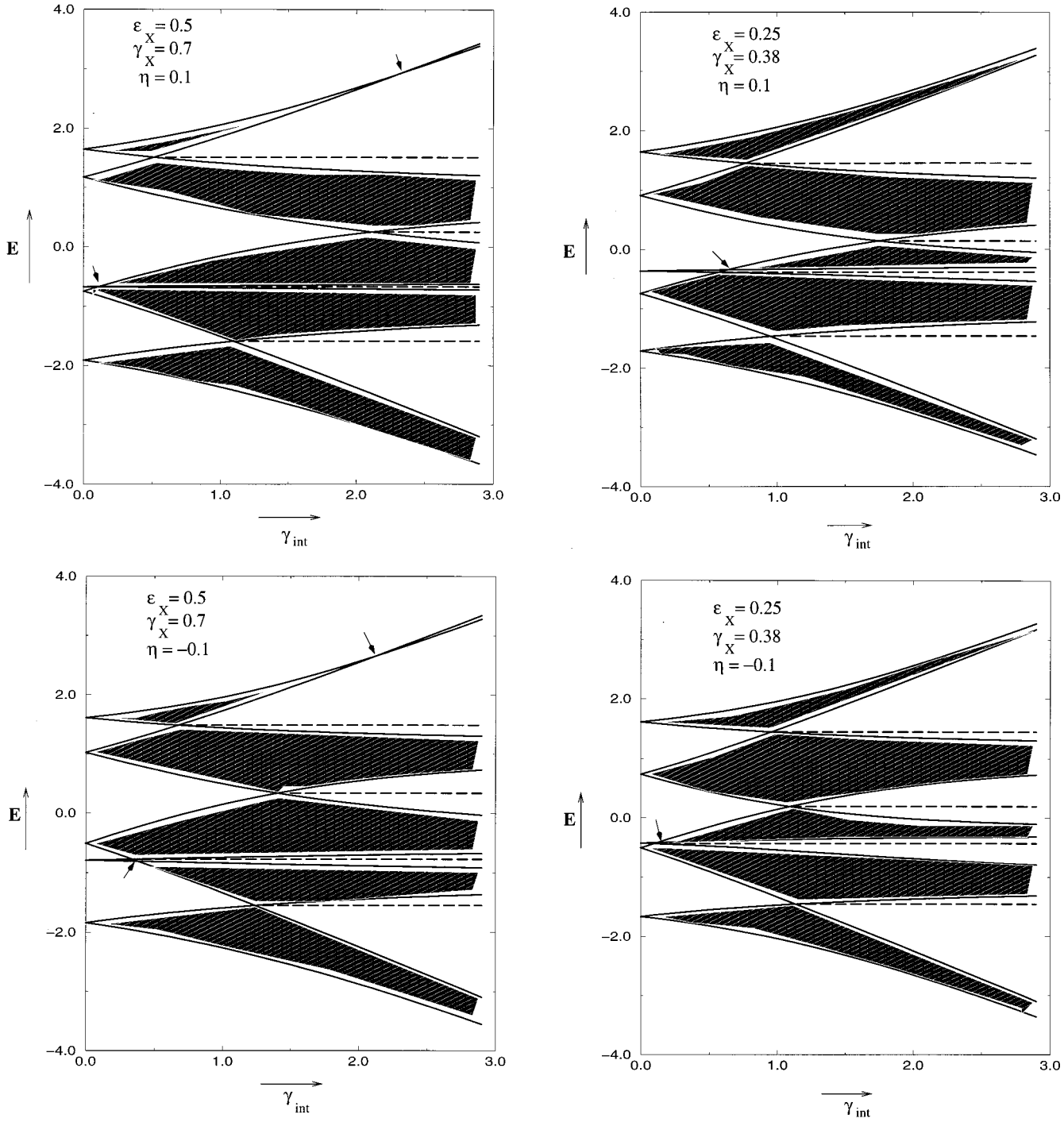

FIG. 4. Gross structure of π electron spectrum of polythiophene as a function of intermonomer resonance interaction γ_{int} calculated for two values of alternation parameter, $\eta = 0.1$ (up) and -0.1 (down), which correspond, respectively, to aromatic and quinoid geometry of carbon backbone (see Fig. 2). Parameters of sulfur are given in Ref. 41. Solid lines start from points $E^M_{i_\pm}$, $i = 1, 2, 3, 4$, and $E^M_{X_\pm}$ on the E axis, which represent energies of monomer levels defined in Eqs. (26)–(28). These lines, which divide the energy interval into allowed (shadowed arrears) and forbidden (blank arrears) zones, correspond to analytical dependences $E_{i_\pm}(\gamma_{\text{int}})$, $i = 1, 2, 3, 4$, and $E_{X_\pm}(\gamma_{\text{int}})$ determined by Eqs. (36)–(39). Dashed lines indicate the position of discrete in-gap levels determined by Eqs. (42) and (44); energies of degenerate bands determined by Eqs. (49) and (50) are indicated by arrows. Energy unit is $|\beta|$, energy reference point—electron site energy (=Coulomb integral) of carbon.

FIG. 5. Same dependences (same values of η and same notations) as in Fig. 4 calculated with the use of sulfur parameters given in Ref. 40.

geometry, both signs of alternation parameter are used with all sets of heteroatom parameters. The equilibrium geometry of heterocyclic polymers is known to be aromatic ($\eta > 0$). The spectra, which correspond to a fixed aromatic conformation of monomers, are shown in the upper parts of Figs. 4–6. However, charging and excitation of conducting polymers lead to the increase of the quinoid character of carbon skeleton ($\eta < 0$). Therefore, the knowledge of π electron spectrum in the case of the quinoid geometry of backbone (lower

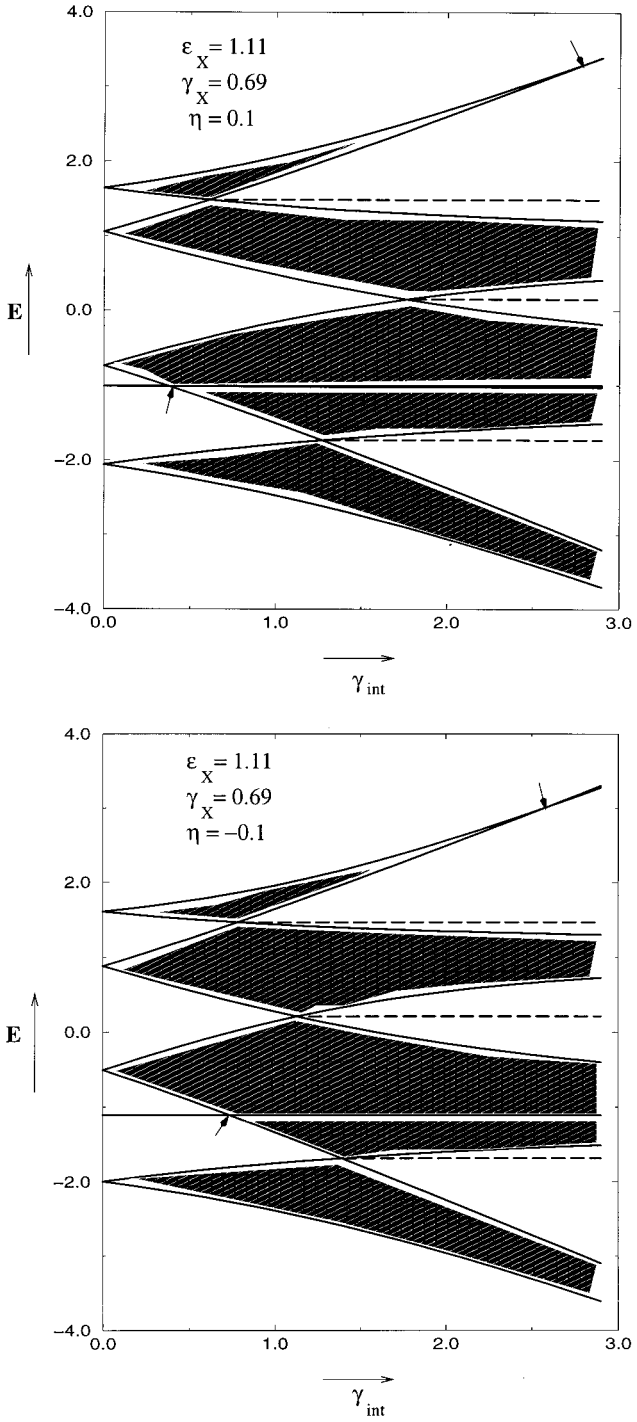

FIG. 6. Same dependences (same values of η and same notations) as in Fig. 4 calculated with the use of sulfur parameters given in Ref. 42.

parts of Figs. 4–6) can be helpful for an estimate of effects which have to be expected under polymer charging and excitation.

A. Polythiophene modeling

Figures 4–6 (see also Tables I and II) represent the π electron spectrum of PTh for fixed values of $\eta=0.1$, -0.1, and three different sets of sulfur parameters: $\epsilon_X=0.5$, $\gamma_X=0.7$ (model I),[41] $\epsilon_X=0.25$, $\gamma_X=0.38$ (model II),[40] and $\epsilon_X=1.11$, $\gamma_X=0.69$ (model III),[42] respectively. We will refer to data calculated with the use of the full set of system parameters given by Birnbaum *et al.*:[40] $\epsilon_X=0.25$, $\gamma_X=0.38$, $\eta=0.1333$,—as model II* (the latter is the only model, where to obtain the characteristic energies in eV, we set $|\beta|=3.757$ eV).[39,40] The ionization potential, electron affinity, bandwidths, band gaps, and positions of discrete in-gap levels calculated for $\gamma_{\rm int}=\exp(-\eta)$ and $\gamma_{\rm int}=1$ are summarized in Table I for aromatic geometry and Table II for quinoid geometry. The former of two indicated values of $\gamma_{\rm int}$ correspond to the ideal sequence of double and single C–C bonds in the carbon backbone. Note that all values in eV given in Tables I and II in parentheses, except for those marked by an asterisk, were obtained under the assumption that $|\beta|=2.75$ eV—a value which is widely used in estimates of energetics of conjugated polymers.

The existence of well defined π bands at small values of intermonomer interaction and their touching at larger values of $\gamma_{\rm int}$ were predicted in the above analytical analysis. An unusual behavior of the band connected with monomer level E_X^M is also implied in the dependence of band-edge energies on $\gamma_{\rm int}$ obtained in Sec. III. It is seen that at certain values of $\gamma_{\rm int}$ [which satisfy Eq. (44)] the X band, which has the smallest bandwidth, touches the nearest C band. At this point a discrete in-gap state appears (because of very small gap between HOMO and HOMO-1 bands $\Delta_{H,H-1}$, a discrete level between upper valence bands is well seen only in Fig. 5). With the further increase of $\gamma_{\rm int}$ the X bandwidth decreases to zero. In Figs. 4–6 the position of $(N-1)$-fold degenerate bands is indicated by arrows. Note that model II and (and II*) predicts the existence of the degenerate band at the value of $\gamma_{\rm int}$, which is not very far from a realistic one (see Fig. 5).

In the case of aromatic geometry all models of PTh used here predict comparatively close dimensionless values of fundamental band gap $\Delta_{H,L}$. For example, at $\gamma_{\rm int}=\exp(-\eta)$ the largest value of $\Delta_{H,L}$ is 0.887, and the smallest one is 0.632. As seen from Table I, with the energy scale used both these values give quite reasonable estimates of $\Delta_{H,L}$ in eV. The excellent fit to the experimental value $\Delta_{H,L}=2$ eV is provided by model III.[44]

The diversity of predictions of models I–III with respect to bandwidths in π electron spectrum of PTh is much larger. In this sense, the comparison with experimental data on bandwidths would be more helpful for making the right choice of model parameters. Unfortunately, relevant experimental data are not available to us.

In agreement with *ab initio* calculations,[8] all three models predict that the conduction bandwidth is larger than the valence bandwidth. However, as is seen from Figs. 4–6 and Table I, models I and III predicts HO (ΔE_H) and LU (ΔE_L) bands to be of comparable widths, whereas model II (and II*) implies a large electron-hole asymmetry: The LU band is by nearly one order wider than the HO band.

It was shown earlier[2,7,9,10] that the increase of quinoid character in the backbone geometry leads to the decrease of fundamental band gap. The dependence of this effect on het-

TABLE I. Main characteristics of π electron spectrum of polythiophene (PTh), polypyrrole (PPy), and polyfuran (PFu). These are ionization potential and electron affinity which are counted from the electron on-site energy at carbon atoms; bandwidths, from up to down: ΔE_{H-2}, ΔE_{H-1}, ΔE_H, ΔE_L, ΔE_{L+1} (ΔE_H and ΔE_L—the widths of the upper valence and lower conduction bands, are underlined); band gaps, from up to down: $\Delta_{H-2,H-1}$, $\Delta_{H-1,H}$, $\Delta_{H,L}$, $\Delta_{L,L+1}$ ($\Delta_{H,L}$—fundamental band gap is underlined); and in-gap discrete levels (counted from the electron on-site energy at carbons). Values of model parameters are indicated in the left hand side column; except data for PTh marked by asterisks, the alternation parameter η was set equal to 0.1, and the energy unit is $|\beta| = 2.75$ eV.

Polymer model (ϵ_X, γ_X)	Ionization potential (HOMO)	Electron affinity (LUMO)	Bandwidths	Band gaps	Local state energies
	in units $\lvert\beta\rvert$ ($\times$2.75 eV)				
PTh					
(I: 0.5, 0.7)					
$\gamma_{int}=1.0$	−0.154 (−0.423)	0.645 (1.772)	0.752 (2.069)	0.105 (0.288)	−0.670 (−1.842)
			0.820 (2.256)	0.035 (0.095)	1.509 (4.149)
			0.498 (1.369)	0.799 (2.195)	
			0.767 (2.109)	0.446 (1.228)	
			0.201 (0.552)		
$\gamma_{int}=0.905$	−0.200 (−0.551)	0.687 (1.891)	0.679 (1.867)	0.206 (0.566)	−0.670 (−1.842)
			0.744 (2.046)	0.031 (0.086)	1.509 (4.149)
			0.453 (1.245)	0.887 (2.442)	
			0.741 (2.037)	0.359 (0.987)	
			0.223 (0.613)		
PTh					
(II: 0.25, 0.38)					
$\gamma_{int}=1.0$	−0.154 (−0.423)	0.392 (1.078)	0.634 (1.745)	0.051 (0.139)	−1.466 (−4.030)
			1.050 (2.888)	0.073 (0.200)	−0.384 (−1.055)
			0.179 (0.493)	0.546 (1.501)	1.455 (4.000)
			1.019 (2.804)	0.223 (0.613)	
			0.424 (1.167)		
$\gamma_{int}=0.905$	−0.200 (−0.551)	0.432 (1.188)	0.617 (1.696)	0.046 (0.127)	−0.384 (−1.055)
			1.028 (2.826)	0.065 (0.179)	1.455 (4.000)
			0.135 (0.371)	0.632 (1.739)	
			0.996 (2.740)	0.132 (0.362)	
			0.450 (1.238)		
PTh					
(II*: 0.25, 0.38)*					
$\gamma_{int}=1.0$	−0.207 (−0.777)	0.428 (1.607)	0.623 (2.342)	0.078 (0.294)	−1.478 (−5.553)
			1.073 (4.031)	0.061 (0.231)	−0.375 (−1.408)
			0.121 (0.455)	0.635 (2.384)	1.467 (5.510)
			0.988 (3.711)	0.249 (0.936)	
			0.417 (1.567)		
$\gamma_{int}=0.875$	−0.267 (−1.005)	0.482 (1.809)	0.610 (2.294)	0.049 (0.183)	−0.375 (−1.408)
			1.056 (3.967)	0.053 (0.200)	1.467 (5.510)
			0.063 (0.236)	0.749 (2.814)	
			0.958 (3.598)	0.129 (0.485)	
			0.449 (1.689)		
PTh					
(III: 1.11, 0.69)					
$\gamma_{int}=1.0$	−0.154 (−0.423)	0.480 (1.321)	0.687 (1.890)	0.281 (0.774)	−1.013 (−2.87)
			0.486 (1.338)	0.010 (0.026)	1.487 (4.090)
			0.857 (2.356)	0.634 (1.744)	
			0.931 (2.560)	0.372 (1.023)	
			0.275 (0.757)		
$\gamma_{int}=0.905$	−0.200 (−0.551)	0.528 (1.447)	0.620 (1.704)	0.381 (1.046)	−1.013 (−2.787)
			0.409 (1.124)	0.009 (0.024)	1.487 (4.090)
			0.811 (2.229)	0.729 (2.004)	
			0.900 (2.475)	0.281 (0.774)	
			0.300 (0.826)		

TABLE I. (*Continued.*)

Polymer model (ϵ_X, γ_X)	Ionization potential (HOMO)	Electron affinity (LUMO)	Bandwidths	Band gaps	Local state energies
	in units $\lvert\beta\rvert$ ($\times 2.75$ eV)				
PPy (I: 1.5, 0.8)					
$\gamma_{\text{int}}=1.0$	-0.154 (-0.423)	0.505 (1.388)	0.611 (1.679) 0.318 (0.874) 0.971 (2.672) 0.906 (2.493) 0.228 (0.627)	0.604 (1.661) 0.064 (0.175) 0.659 (1.811) 0.419 (1.153)	-1.139 (-3.131) 1.498 (4.119)
$\gamma_{\text{int}}=0.905$	-0.200 (-0.551)	0.555 (1.526)	0.550 (1.513) 0.243 (0.668) 0.928 (2.551) 0.873 (2.402) 0.253 (0.696)	0.700 (1.926) 0.058 (0.158) 0.755 (2.077) 0.328 (0.903)	-1.139 (-3.131) 1.498 (4.119)
PPy (II: 1.37, 1.27)					
$\gamma_{\text{int}}=1.0$	-0.154 (-0.423)	1.001 (2.753)	0.713 (1.961) 0.474 (1.304) 0.861 (2.368) 0.410 (1.128) 0.212 (0.583)	1.024 (2.816) 0.017 (0.048) 1.155 (3.176) 0.647 (1.780)	-1.020 (-2.805) 1.626 (4.472)
$\gamma_{\text{int}}=0.905$	-0.200 (-0.551)	1.052 (2.892)	0.644 (1.772) 0.397 (1.092) 0.815 (2.242) 0.377 (1.036) 0.191 (0.526)	1.127 (3.100) 0.016 (0.043) 1.252 (3.443) 0.582 (1.600)	-1.020 (-2.805) 1.626 (4.472)
PFu (2.0, 0.8)					
$\gamma_{\text{int}}=1.0$	-0.154 (-0.423)	0.436 (1.199)	0.473 (1.302) 0.113 (0.312) 1.067 (2.935) 0.975 (2.682) 0.268 (0.737)	0.968 (2.662) 0.172 (0.473) 0.590 (1.622) 0.379 (1.043)	-1.243 (-3.419) 1.487 (4.090)
$\gamma_{\text{int}}=0.905$	-0.200 (-0.551)	0.488 (1.340)	0.425 (1.170) 0.045 (0.124) 1.027 (2.824) 0.941 (2.588) 0.295 (0.810)	1.060 (2.915) 0.156 (0.429) 0.688 (1.891) 0.287 (0.790)	-1.243 (-3.419) 1.487 (4.090)

*These data are calculated with parameters given by Birnbaum, Kohler, and Spangler (Ref. 33): $\epsilon_X=0.25$, $\gamma_X=0.38$, $\eta=0.133$, and $\lvert\beta\rvert=30305\ \text{cm}^{-1}=3.757$ eV.

eroatom parameters is well illustrated by the given and forthcoming examples. One can see that a quantitative estimate of geometry effects on the band gap, as well as on other characteristics of π electron spectrum, are crucially dependent on the precise position of heteroatom level and the strength of its resonance interaction with alpha carbons. For example, model I predicts that passing from aromatic to quinoid geometry results in a comparatively moderate decrease of $\Delta_{H,L}$ which is not very sensitive to the choice of γ_{int}. By contrast, models II and III give up to more than by an order decrease of this quantity and predict a strong dependence of the effect on the intermonomer interaction. The reasons for this difference in predictions can be seen from the structure of π electron spectra displayed in Figs. 4–6.

The effect produced by changing geometry on the width of π bands also reveals a significant dependence on heteroatom parameters. For instance, models I and III predict an overall moderate increase of ΔE_H and ΔE_L (larger for ΔE_H, than for ΔE_L, that is with tendency to the equalization widths of electron and hole bands), whereas accordingly to model II, the increase of the HO bandwidth must be anomalously large and very sensitive to the effective value of intermonomer resonance interaction.

As it is implied by the model Hamiltonian and equilibrium geometry, ionization potential (top of HO band) does not depend on heteroatom parameters. For this reason the corresponding data presented in Tables I and II are identical for all heterocyclic polymers. This suggests therefore, that in the framework of the given model, the experimentally observed difference in ionization potentials of PTh, PPy, and PFu has to be associated with distinctions in carbon backbones of these polymers. It is also worth mentioning that

TABLE II. Same data as in Table I calculated with the same parameters but under the assumption of the quinoid geometry of carbon backbone, i.e., η is replaced by $-\eta$.

Polymer model (ϵ_X, γ_X)	Ionization potential (HOMO)	Electron affinity (LUMO)	Bandwidths	Band gaps	Local state energies
	in units $\lvert\beta\rvert$ ($\times 2.75$ eV)				
PTh					
(I: 0.5, 0.7)					
$\gamma_{int}=1.0$	0.146 (0.402)	0.497 (1.363)	0.673 (1.852)	0.254 (0.699)	-0.774 (-2.128)
			0.498 (1.368)	0.094 (0.257)	1.484 (4.082)
			0.890 (2.449)	0.349 (0.961)	
			0.945 (2.599)	0.288 (0.792)	
			0.239 (0.633)		
$\gamma_{int}=1.105$	0.200 (0.551)	0.451 (1.241)	0.748 (2.058)	0.142 (0.391)	-0.774 (-2.128)
			0.586 (1.610)	0.103 (0.283)	1.484 (4.082)
			0.940 (2.585)	0.251 (0.690)	
			0.977 (2.687)	0.382 (1.050)	
			0.200 (0.551)		
PTh					
(II: 0.25, 0.38)					
$\gamma_{int}=1.0$	0.146 (0.402)	0.224 (0.617)	0.567 (1.560)	0.136 (0.374)	-0.435 (-1.196)
			0.794 (2.185)	0.174 (0.479)	1.446 (3.977)
			0.513 (1.410)	0.078 (0.215)	
			1.216 (3.344)	0.042 (0.116)	
			0.476 (1.309)		
$\gamma_{int}=1.105$	0.188 (0.516)	0.201 (0.551)	0.634 (1.744)	0.029 (0.080)	-0.435 (-1.196)
			0.872 (2.398)	0.194 (0.533)	0.193 (0.530)
			0.550 (1.513)	0.013 (0.035)	1.446 (3.977)
			1.228 (3.377)	0.142 (0.389)	
			0.440 (1.210)		
PTh					
(II*: 0.25, 0.38)*					
$\gamma_{int}=1.0$	0.193 (0.726)	0.204 (768)	0.545 (2.046)	0.171 (0.643)	-0.443 (-1.664)
			0.743 (2.791)	0.197 (0.740)	1.456 (5.469)
			0.565 (2.124)	0.011 (0.042)	
			1.250 (4.697)	0.008 (0.030)	
			0.487 (1.829)		
$\gamma_{int}=1.143$	0.157 (0.589)	0.268 (1.004)	0.634 (2.381)	0.026 (0.099)	-0.443 (-1.664)
			0.847 (3.181)	0.227 (0.852)	0.200 (0.751)
			0.523 (1.963)	0.111 (0.415)	1.456 (5.469)
			1.172 (4.403)	0.142 (0.534)	
			0.436 (1.639)		
PTh					
(III: 1.11, 0.69)					
$\gamma_{int}=1.0$	0.146 (0.402)	0.278 (0.764)	0.634 (1.744)	0.416 (1.144)	-1.107 (-3.045)
			0.228 (0.627)	0.000 (0.000)	1.469(4.040)
			1.254 (3.447)	0.132 (0.362)	
			1.163 (3.197)	0.203 (0.558)	
			0.315 (0.867)		
$\gamma_{int}=1.105$	0.200 (0.551)	0.224 (0.617)	0.705 (1.939)	0.304 (0.835)	-1.107 (-3.045)
			0.321 (0.883)	$0.72\cdot 10^{-5}$ ($0.20\cdot 10^{-4}$)	1.469 (4.040)
			1.308 (3.596)	0.024 (0.066)	
			1.204 (3.311)	0.301 (0.828)	
			0.281 (0.772)		
PPy					
(I: 1.5, 0.8)					
$\gamma_{int}=1.0$	0.146 (0.402)	0.296 (0.815)	0.573 (1.575)	0.739 (2.031)	-1.226 (-3.372)
			0.081 (0.222)	0.030 (0.084)	1.476 (4.060)
			1.371 (3.769)	0.150 (0.413)	
			1.144 (3.146)	0.253 (0.695)	
			0.266 (0.730)		
$\gamma_{int}=1.105$	0.200 (0.551)	0.239 (0.659)	0.637 (1.752)	0.628 (1.727)	-1.226 (-3.372)
			0.172 (0.472)	0.034 (0.092)	1.476 (4.060)
			1.423 (3.914)	0.039 (0.108)	

TABLE II. (*Continued.*)

Polymer model (ϵ_X, γ_X)	Ionization potential (HOMO)	Electron affinity (LUMO)	Bandwidths	Band gaps	Local state energies
	in units $\lvert\beta\rvert$ ($\times 2.75$ eV)				
			1.189 (3.269)	0.351 (0.965)	
			0.231 (0.634)		
PPy					
(II: 1.37, 1.27)					
$\gamma_{\text{int}}=1.0$	0.146 (0.402)	0.861 (2.370)	0.693 (1.906)	1.150 (3.162)	-1.154 (-3.173)
			0.177 (0.487)	0.005 (0.014)	1.574 (4.328)
			1.299 (3.574)	0.715 (1.968)	
			0.579 (1.592)	0.518 (1.425)	
			0.204 (0.562)		
$\gamma_{\text{int}}=1.105$	0.200 (0.551)	0.805 (2.216)	0.768 (2.112)	1.031 (2.836)	-1.154 (-3.173)
			0.270 (0.742)	0.006 (0.016)	1.574 (4.328)
			1.353 (3.722)	0.605 (1.665)	
			0.623 (1.712)	0.582 (1.600)	
			0.233 (0.640)		
PFu					
(2.0, 0.8)					
$\gamma_{\text{int}}=1.0$	0.146 (0.042)	0.205 (0.564)	0.442 (1.215)	1.032 (2.839)	-1.304 (-3.587)
			0.083 (0.227)	0.032 (0.089)	1.469 (4.040)
			1.449 (3.985)	0.059 (0.162)	
			1.235 (3.397)	0.208 (0.571)	
			0.311 (0.855)		
$\gamma_{\text{int}}=1.105$	0.146 (0.402)	0.201 (0.552)	0.493 (1.355)	1.009 (2.774)	-1.304 (-3.587)
			0.002 (0.006)	0.127 (0.350)	0.174 (0.480)
			1.445 (3.973)	0.055 (0.150)	1.469 (4.040)
			1.228 (3.377)	0.308 (0.846)	
			0.274 (0.754)		

using electronegativity of carbons ($=6.26$ eV)[45] as the energy reference point and value -0.551 eV for ionization potential (IP) from Table I one obtains IP$=6.81$ eV, which is in a very good agreement with the ''experimental'' estimate of this quantity for PTh given in Ref. 13.

B. Polypyrrole modeling

Two sets of parameters $\epsilon_X=1.5$, $\gamma_X=0.8$;[43] and $\epsilon_X=1.37$, $\gamma_X=1.27$ (Ref. 10) (with $\eta=\pm 0.1$) hereinafter referred as models I and II of PPy, respectively, have been used to mimic the π electron spectrum of this polymer. The best fit to experimentally observed value $\Delta_{H,L}=3.2$ eV (Ref. 46) gives model II, see Table I. The latter model also predicts a substantially lower electron affinity of PPy, than that of PTh in agreement with experimental results.

Models I and II diverge in their predictions concerning electronic structure of PPy quite significantly. In particular, model I gives nearly equal values of ΔE_H and ΔE_L, whereas model II implies a two times larger value of the valence bandwidth. It is interesting to note that models II, II* of PTh predict the reversed electron-hole asymmetry. Also, model I predicts a very strong reduction of $\Delta_{H,L}$ with the increase of the quinoid character of carbon backbone, while accordingly to model II, this effect has to be much weaker. By comparing these and other predictions with a sufficient wealth of experimental data it seems possible to make the right choice of basic parameters of PPy and thus, to get into microscopic origins of π electronic structure of PPy and similar polymers.

C. Polyfuran modeling

The use of model I with ''standard'' Hückel parameters, represented by spectra of PTh and PPy is continued by calculations of the gross structure of PFu π electron spectrum, see Tables I and II. As it was indicated above model I does not provide coincidence of theory predictions with known experimental results for PTh and PPy, at least without additional assumptions with respect to the intermonomer interaction. The given model of PFu ($\epsilon_X=2.0$, $\gamma_X=0.8$)[43] also leads to a divergence with experimental data. This cannot be considered, of course, as an argument for rejecting this approach but rather as an accentuation of importance of the consistent choice of system parameters.

Since the applicability of the given model is doubtful, the reason for its representation here is to illustrate the dependence of heteroatom effects on the electron site energy at heteroatom. Indeed, since in model I all other parameters except ϵ_X are essentially the same, the results obtained for PTh, PPy, and PFu give a detailed picture of the evolution of heteroatom effects with the increase of ϵ_X. It is seen, in particular, that changes in the heteroatom site energy are reflected mostly in the relative position and widths of va-

lence bands, while the conduction bands are much less affected. With the increase of ϵ_X the energy of the lowest valence band considerably decreases. This lowering is much larger than an upward shift of the upper valence band. It is also interesting to note that for the largest used value of ϵ_X the degeneracy of the middle valence band is realized near $\gamma_{\text{int}}=0.9$, where $\Delta E_{H-1}=0.045$ (see Table I).

V. CONCLUDING REMARKS

Starting from the SSH Hückel type Hamiltonian which is appropriately generalized to account for the electronic structure of five-membered heterocycles (thiophene, pyrrole, and furan) the one-electron theory of corresponding polymers with rigid backbone has been developed.

It is shown that π-band joining (gap closing) and the appearance of in-gap discrete levels are determined by zeros of monomer Green function diagonal component referred to binding sites at which monomers are connected to each other by covalent bonds. Thus, the closing of any gap in polymer spectrum occurs at the energy which is a reflection of monomer nature. This energy is independent of intermonomer interaction but how far or close the given gap is from zero value does depend on the magnitude of intermonomer resonance interaction (γ_{int}) which is realized in the polymer.

The necessary and sufficient condition of gap closing in the spectrum of heterocyclic polymers (expressed as a relation between the monomer and intermonomer-interaction parameters) is given by Eq. (44). Each gap closes at a certain value of γ_{int} determined by the above mentioned relation. If the intermonomer interaction is smaller or larger than the value predicted by Eq. (44), the gap is nonzero i.e., the corresponding adjacent π bands are separated by a forbidden zone. At larger values of γ_{int}, there is a doubly degenerate discrete level within this zone. In the other words, π band joining gives rise to a local state. Both features, band joining and appearance of discrete levels at the sufficiently large strength of intermonomer interaction, are inherent properties of conjugated polymers.

It is demonstrated that unlike six-membered based polymers, where the existence of degenerate bands is connected with monomer eigenstates having nodes at binding sites, in heterocyclic polymers there exists an additional possibility of band degeneracy at certain values of intermonomer interaction. The energies of degenerate bands are determined by zeros of the nondiagonal component of monomer Green function and thus, these are also a reflection of internal monomer structure. The relation between the system parameters, the fulfillment of which is the necessary and sufficient condition of the presence of degenerate band in the polymer spectrum, is given by Eq. (50) (several equivalent forms of this equation are possible).[47] Some sets of Hückel parameters which are suggested in the literature to model heteroatoms, are found to be very close to fulfilling the above mentioned condition.

In the framework of the accepted model, it is proved that four of 10 band-edge energies of π electron spectrum of heterocyclic polymers are not affected by heteroatom–carbon resonance interaction due to the fact that the corresponding edge states in the polymer have the symmetry of monomer eigenstates. The exact explicit expressions of all band-edge energies as functions of system parameters are found. The closed expressions of orthonormalized molecular orbitals of heterocyclic oligomers/polymers are also presented here for the first time.

Together with other conclusions made throughout the analytical analysis and discussion of illustrative examples, the theoretical results outlined above reveal a lot of new physics of this class of conjugated polymers which deserves experimental testing.

The theory developed has been applied to the description of the gross structure of heterocyclic polymers with the use of Hückel parameters suggested in literature for heteroatoms—sulfur, nitrogen, and oxygen. Despite the uncertainty of these parameters, the encouraging fact is that with a reasonable choice of system parameters an excellent agreement with experimental data can be achieved as is demonstrated for the fundamental band gaps of polythiophene and polypyrrole. This rises to a challenge of consistent experimental determination of model parameters which can certainly be met in wide-scale spectroscopic measurements.

ACKNOWLEDGMENTS

This work was supported in part by the Swiss National Science Foundation under the program CEEC/NIS. A.I.O. is thankful for a grant from the Swedish Foundation for International Cooperation in Research and Higher Education.

[1] W. K. Ford, C. B. Duke, and W. R. Salaneck, J. Chem. Phys. **77**, 5030 (1982).
[2] J. L. Brédas, B. Thémans, J. G. Fripiat, and J. M. André, Phys. Rev. B **29**, 6761 (1984).
[3] J. L. Brédas, J. Chem. Phys. **82**, 3808 (1985).
[4] J. L. Brédas, G. B. Street, B. Thémans, and J. M. André, J. Chem. Phys. **83**, 1323 (1985).
[5] O. Wennerström, Macromolecules **18**, 1977 (1985).
[6] J. L. Brédas, A. J. Heeger, and F. Wudl, J. Chem. Phys. **85**, 4673 (1986).
[7] J. W. Mintmire, C. T. White, and M. L. Elert, Synth. Met. **16**, 235 (1986).
[8] A. K. Bakhshi, J. Ladik, and M. Seel, Phys. Rev. B **35**, 704 (1987).
[9] J. L. Brédas, Synth. Met. **17**, 115 (1987).
[10] Y.-S. Lee and M. Kertesz, J. Phys. Chem. **88**, 2609 (1988).
[11] S. Stafström and J. L. Brédas, J. Mol. Struct. **188**, 393 (1989).
[12] J. L. Brédas and A. J. Heeger, Macromolecules **23**, 1150 (1990).
[13] D. Jones, M. Guerra, L. Favaretto, A. Modelli, M. Fabrizio, and G. Distefano, J. Phys. Chem. **94**, 5761 (1990).
[14] S. Y. Hong and D. S. Marynick, J. Phys. Chem. **96**, 5497 (1992).
[15] J. Cornil, D. Beljonne, and J. L. Brédas, J. Chem. Phys. **103**, 842 (1995).
[16] S. Y. Hong, Bull. Korean Chem. Soc. **16**, 845 (1995).
[17] A. J. Heeger, S. Kivelson, J. R. Schrieffer, and W.-P. Su, Rev. Mod. Phys. **60**, 781 (1988).
[18] W. P. Su, J. R. Schrieffer, and A. J. Heeger, Phys. Rev. Lett. B **42**, 1698 (1979); Phys. Rev. B **22**, 1099 (1980).
[19] S. Brazovskii and N. Kirova, Zh. Eksp. Teor. Fiz. Pis'ma Red. **33**, 6 (1981) [JETP Lett. **33**, 4 (1981)].
[20] K. Fesser, A. R. Bishop, and D. K. Campbell, Phys. Rev. B **27**, 4804 (1983).
[21] S. Stafström and J. L. Brédas, Phys. Rev. B **38**, 4180 (1988).
[22] Ch. Ehrendorfer and A. Karpfen, J. Phys. Chem. **98**, 7492 (1994).
[23] A. J. W. Tol, Synth. Met. **74**, 95 (1995).
[24] D. Giri and K. Kundu, Phys. Rev. B **53**, 4340 (1996).
[25] S. Kivelson and A. J. Heeger, Phys. Rev. Lett. **85**, 308 (1985).

[26] F. C. Lavarda, M. C. dos Santos, D. S. Galvão, and B. Laks, Phys. Rev. B **49**, 979 (1994).
[27] K. Kundu and D. Giri, J. Chem. Phys. **105**, 11075 (1996).
[28] I. M. Lifshits, Zh. Eksp. i Teor. Fiz. **17**, 1017; 1076 (1947).
[29] G. F. Koster and J. C. Slater, Phys. Rev. **95**, 1167 (1954).
[30] Y. Jido, T. Inagaki, and H. Fukutome, Progr. Theor. Phys. **48**, 808 (1972).
[31] M. V. Kaulgud and V. H. Chitgopkar, J. Chem. Soc. Faradey Trans. II **73**, 1385 (1977).
[32] J. Koutesky, Advan. Chem. Phys. **9**, 85 (1965).
[33] G. F. Kventsel, Teoret. Experim. Khim. **4**, 291 (1968); **5**, 26 (1969).
[34] O. Castaño and P. Karadakov, Z. Phys. Chem. N. F. **126**, 205 (1981).
[35] S. Larsson and M. Braga, Chem. Phys. **176**, 367 (1993).
[36] Y. Y. Suzuki and J. L. Brédas, Phys. Scr. **49**, 509 (1994).
[37] Y. Y. Suzuki, D. Beljonne, and J. L. Brédas, J. Chem. Phys. **104**, 7270 (1996).
[38] L. I. Malysheva and A. I. Onipko, Synth. Met. **80**, 11 (1996); J. Chem. Phys. **105**, 11032 (1996).
[39] B. E. Kohler, J. Chem. Phys. **93**, 5838 (1990).
[40] D. Birnbaum, B. E. Kohler, and C. W. Spangler, J. Chem. Phys. **94**, 1684 (1991).
[41] J. Fabian, in *Sulfur in Organic and Inorganic Chemistry*, edited by A. Senning (Marcel Dekker, New York, 1972), Vol. 3, pp. 39–90.
[42] F. A. Van-Catledge, J. Org. Chem. **45**, 4801 (1980).
[43] A. Streitwieser, Jr., *Molecular Orbital Theory* (Wiley, New York, 1961).
[44] K. Kaneto, K. Yoshino, and Y. Inuishi, Solid State Commun. **46**, 389 (1983).
[45] J. N. Murrell, S. F. Kettle, and J. M. Tedder, *The Chemical Bond* (Wiley, Chichester, 1985).
[46] G. B. Street, T. C. Clarke, M. Krounbi, K. K. Kanazawa, V. Y. Lee, P. Pfluger, J. C. Scott, and G. Weiser, Mol. Cryst. Liq. Cryst. **83**, 253 (1982).
[47] In this presentation a number of interesting mathematical details have been omitted for the sake of brevity. These can be provided by the authors on request.